processes

MDPI

Article

Thermal Pyrolysis of Polystyrene Aided by a Nitroxide End-Functionality. Experiments and Modeling

Almendra Ordaz-Quintero, Antonio Monroy-Alonso and Enrique Saldívar-Guerra *

Centro de Investigación en Química Aplicada, Blvd. Enrique Reyna 140, Saltillo Coahuila 25294, Mexico; almendra.ordaz@ciqa.edu.mx (A.O.-Q.); antonio.monroy.alonso@hotmail.com (A.M.-A.)

* Correspondence: enrique.saldivar@ciqa.edu.mx; Tel.: +52-844-439-4408

Received: 27 February 2020; Accepted: 31 March 2020; Published: 5 April 2020

Abstract: The thermal pyrolysis of polystyrene (PS) is gaining importance as the social pressure for achieving a circular economy is growing; moreover, the recovery of styrene monomer in such a process is especially relevant. In this study, a simple thermal pyrolysis process in the temperature range of 390–450 °C is developed. A working hypothesis is that by using a nitroxide-end functionalized PS (PS-T or dormant polymer), the initiation process for the production of monomer (unzipping) during the PS pyrolysis could be enhanced due to the tendency of the PS-T to activate at the nitroxide end. Two types of PS were used in this work, the first one was synthesized by free-radical polymerization (FRP-dead polymer) and the second by nitroxide-mediated polymerization (NMP) using three levels of nitroxide to initiator ratio: 1.3, 1.1, and 0.9. Analysis of the recovered products of the pyrolysis by gas-mass spectroscopy shows that the yield of styrene increases from ~33% in the case of dead polymer to ~38.5% for PS-T. A kinetic and mathematical model for the pyrolysis of dead and dormant polymer is proposed and solved by the method of moments. After a parameter sensitivity study and data fitting, the model is capable of explaining the main experimental trends observed.

Keywords: polystyrene; thermal pyrolysis; nitroxide mediated polymerization; mathematical modeling

1. Introduction

Plastics are widely used materials due to their physical and chemical properties; [1] additionally, they are cheap, light, long-lasting [2], and relatively easy to produce [3]. These outstanding properties are the ones that have led to their excessive production and irresponsible consumption, originating severe ecological problems that could cause irreversible damage to the environment [4–6].

Essentially there are three traditional solutions for plastic waste management, each one presenting significant drawbacks: Landfill disposal, recycling, and combustion [6]. In landfill disposal, none of the material resources used to produce plastics are recovered. With respect to the second alternative, the recycling capacity of polymers is inherently limited since after a determined number of recycling processes the materials exhibit reduced mechanical properties and the plastic ends up being thrown away. Regarding the third option, recovering energy from combustion is feasible, but it causes negative effects on the environment and human health.

Given the increasing social pressure to take care of the environment and the present trends towards circular economy, a better option to manage plastic waste would be to transform it into defined chemical compounds, especially the source monomer, with the required purity and quality to be used again as raw material in the same polymerization or in other processes. One such technique that permits the recovery of high-value compounds is pyrolysis, which can be finely tuned to favor

some product distribution over others. The practical implementation of a chemical recycling strategy requires a concerted effort among different sectors of the society (the general population, municipal governments, polymer producers, and recycling companies), but there are already some successful examples of this model.

Pyrolysis of plastics can be carried out via thermal or catalytic routes, and the distribution of obtained products is influenced by a wide range of parameters, including the type of waste used, the type of reaction system, the residence time, the pressure range, the presence or absence of catalysts, the presence of hydrogen donor compounds, and several others that affect the composition and yield of the obtained products, which consist of complex mixtures that require further separation if individual products are desired.

Purely thermal pyrolysis processes temperatures can reach up to 900 °C which enhance the rate of secondary decomposition reactions and reduce the liquid yield, producing low-quality products with no predictable composition of a broad range of compounds [7]. Catalytic pyrolysis, on the other hand, promotes the polymer decomposition at lower temperatures and shorter times, reducing the energy consumption and enhancing the selectivity of the obtained products, but implying extra costs of the catalyst and its regeneration. In the case of the present proposed process, despite the reactions taking place purely thermally (with temperatures above, but close to the ceiling point of polystyrene), the obtained distribution of products shows a selectivity similar to that of a catalytic process.

Submitting polymers to heat deeply alters their main chain structure, their substituent atoms, and their side chains, provoking random scission at weak links in the main chain, at a chain-end, or in labile structures and, depending on the site of reaction in the polymer structure and the conditions chosen for the particular system, the resulting radicals follow different paths of reaction, from depolymerization of the main chain to inter- or intramolecular transfer reactions [8].

The pyrolysis of pyrolysis of polystyrene (PS) has been a topic of interest for many years, and it is not surprising that renewed interest is rising considering all of the above trends and given that PS is a thermoplastic used throughout the world in a variety of applications.

Thermal degradation of PS is considered to be a chain radical process [9–11], but despite numerous studies and experiments performed to understand its mechanism, many aspects of the problem remain unresolved, making it still difficult to accurately predict the product distribution at a given set of conditions. Additionally, as the process system temperature increases, so does its complexity [8].

The recovery of styrene monomer in the highest possible yield is a desired output of the pyrolysis process of PS, since this would contribute to the consolidation of a circular economy. Therefore, any effort directed towards this goal should be welcome. It is our hypothesis that modifying PS with a nitroxide moiety at a chain-end could enhance the generation of monomer when this material is subjected to thermal pyrolysis at a temperature higher than the ceiling temperature of PS. In this paper, empirical evidence that supports this hypothesis is presented and a mechanistic and mathematical model that is consistent with the experimental observations is also presented and discussed. Before that, background information that supports and motivates this hypothesis is introduced. In the next paragraphs, a brief literature review is made, including a description of the reaction mechanism and previous experimental work. Some of the studies are of academic nature, while many others are associated with patents.

Reaction Mechanism. It has been reported that the molecular weight of polystyrene decreases on heating in vacuum at 250 °C, and when heated above 300 °C volatile products are formed [8,10]. With regard to the initiation process, it is accepted that the radicals are formed by different mechanisms such as chain-end initiation, random mid-chain scission, and scission at irregular structures or "weak links" distributed along the polymer chain such as head-to-head linkages, chain branches, and unsaturated bonds [9,10,12,13]. Lehrle et al. [13] concluded that between 450 to 480 °C initiation occurs both by random mid-chain scission and at chain-ends, and Madorsky [14] pointed out that between 300 to 400 °C it degrades preferably at the ends and that simultaneously some random degradation takes place.

Propagation reactions include intramolecular transfer, which involves the transfer of a hydrogen atom within a single polymer chain and intermolecular hydrogen transfer, comprising the transfer of a hydrogen atom between polymer chains. Also included in this category is the depropagation reaction, where no hydrogen transfer occurs; this reaction is essentially the reverse of the polymerization propagation, also called unzipping or depolymerization, and is mainly responsible for the production of styrene monomer [10,15].

It has been claimed that the most frequent propagation reaction taking place in the 280–350 °C temperature range is β-scission [9], either at a reaction end or at a mid-chain position, a reversible reaction that becomes faster as the ceiling temperature is approached (310–390 °C depending on the source [16,17]); below 300 °C the production of styrene is hardly observed. The second most important reaction is the hydrogen abstraction from the main chain by any radical, producing a saturated chain-end from the attacking radical, and a new radical that undergoes β-scission [9]. At higher temperatures (600 and 700 °C), increased production of benzene, toluene, ethylbenzene, and α-methyl styrene and decreased production of styrene have been observed, probably due to the predominance of intramolecular hydrogen transfer reactions at this range of temperatures [18]. Concerning termination, some authors propose a mechanism involving the recombination [9,11], or the disproportionation reaction [19] between two radicals; while others suggest the occurrence of depropagation until the end of the polymer molecule [13].

Published studies related to the thermal degradation and pyrolysis of polystyrene [13,20–25] have been performed in a variety of reaction systems and sets of conditions, including reaction temperatures, reaction times, and molecular weights of the polystyrene sample, resulting in a broad collection of reaction yields and product distribution. The available reported experimental data fall into three types: chemical nature of the products (that help to elucidate the degradation mechanism), rate of evolution of products, and the change of molecular weight in the residue.

Jellinek [22] reported experiments carried out in long open-to-air tubes containing 0.1 to 0.5 g of material, to show the influence of oxygen on the thermal degradation of polystyrene. The reactions were described as too violent above 220 °C, many side reactions set in and the material quickly became yellow and brown. They assumed that the first stage of the oxidation consisted of the formation of hydro peroxide groups, which led to chain scission, and that at later stages, the reaction slowed down due to the formation of antioxidants such as benzaldehyde. For practical application, to avoid the presence of oxygen in the resulting products, pyrolysis processes are designed to occur in an inert atmosphere. Ebert et al. [23] pyrolyzed samples of polydisperse polystyrene with molecular weights between 60,000 and 220,000 Da in ampoules free of oxygen at temperatures between 270 and 336 °C, assessing the sample weight loss as a function of degradation time. They also performed simulations of the thermal degradation assuming that scission and unzipping occur independently, and attributed scission as the main cause for the decrease in molecular weight, while unzipping as the sole cause of volatiles production. Additionally, in oxygen-free glass ampoules, Wegner and Patat [26] analyzed n-butyl lithium initiated polystyrene samples with molecular weights between 110,000 to 900,000 Da, submitting them to temperatures between 200 to 325 °C, concluding that the polystyrene molecule does not contain thermolabile bonds corresponding to the weak-links theory.

Reactions conducted in a fluidized-bed reactor with operation temperatures in the range 450–700 °C, nitrogen atmosphere, heated by an external electric furnace, permitted liquid recovery above 90%, with the main components being styrene monomer, dimer and trimer, benzene, toluene, ethylbenzene, and α-methyl styrene [20].

Simard et al. [21] reported PS pyrolysis experiments using flat bottom vessels and temperatures between 370–420 °C, with a maximum reaction time of 45 min, observing that 85 to 95% of the obtained liquid fraction are styrene, dimer, and trimer. Anderson and Freeman [25] assessed the weight loss of samples heated from 246 to 430 °C, observing decomposition at 320 °C and 99% of weight loss at 430 °C.

Small scale PS pyrolysis experiments have also been performed. Richards and Salter [24] intentionally synthesized polystyrene containing weak links in its structure that differ from the usual head–tail links of the polymer backbone and should, therefore, have different thermal properties. The pyrolysis experiments were performed at 276–329 °C, and the main product from both polymers was styrene, although significant quantities of dimer and trimer were also formed, the main difference being that the molecular weight of the polymer with weak links decreased more rapidly.

Several patents regarding polystyrene pyrolysis have also been filed [27–32] reporting the use of temperatures varying in a wide range, 330–870 °C, styrene monomer recovery from 33 to 80%, and diverse processes, including the use of a fluidized bed reactor [31] and the use of solvents like toluene [32].

In general, pyrolysis temperature is a very important factor affecting the product distribution [20]; in all the studies both higher temperatures and longer reaction times resulted in an increase in the amount of the liquid yield [21] and a decrease in the molecular weight of the residue. Many of these experiments were done with very small samples (micrograms and milligrams) and none of them had an initial charge greater than 25 g. At increasing temperatures more monomer is formed reaching a maximum at 600 °C where secondary reactions take place.

As can be seen, the use of solvents and catalytic systems allows high yield of styrene recovery, although some drawbacks associated with these processes are evident, such as high operating temperatures and a wide range of obtained products by purely thermal pyrolysis.

On the other hand, nitroxide-mediated polymerization (NMP) is among the most popular techniques in the category of RDRP (reversible deactivation radical polymerization) that provide living character to free radical polymerizations and control the structure of the resulting polymers, enabling the production of polymers with narrow molecular weight distributions and the formation of well-defined polymer architectures such as block copolymers [33]. Roughly speaking, these techniques simultaneously provide some of the advantages of living polymerizations (structure control) and conventional radical polymerization (robustness to impurities and to protic media). NMP, which is especially suited for styrene polymerization, is based on a reversible termination mechanism between the propagating growing species and a stable free radical (nitroxide radical), that acts as a control agent to generate a macro alkoxyamine (dormant polymer) as predominant species. The dormant polymer eventually regenerates a propagating radical and a nitroxide radical through a homolytic breakage as the dormant and the radical species are in dynamic equilibrium resulting from the reversible deactivation-activation reactions just described (see Figure 1). As a result of the NMP process, the final product is mainly constituted by dormant polymer end-functionalized with a nitroxide moiety. For most practical purposes this polymer can be prepared to be very similar to the product produced via conventional free-radical polymerization (except for its dispersity). However, its nitroxide-end functionality should make it more favorable to depolymerization in a certain range of temperatures (via unzipping) than the conventional PS, due to the increased possibility of chain-end initiation of the depolymerization reaction via rupture of the oxygen–carbon bond between the nitroxide moiety and the rest of the polymeric chain.

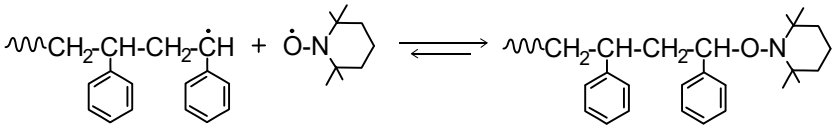

Figure 1. Depolymerization initiation reaction via oxygen–carbon bond rupture (nitroxide radical activation/deactivation).

With respect to the thermal pyrolysis process, it is known that chain-end initiation in mild temperature conditions or moderately above the polystyrene ceiling temperature (310 °C) leads to unzipping and increased production of styrene monomer over other products of this process.

Roland and Schmidt-Naake [34] studied the polymerization of styrene with TEMPO and benzoyl peroxide, claiming that the reversible capping with TEMPO can introduce a weak link at the end of the polymer, such as the bond between polymer and nitroxide. They conclude that polymer degradation for this material occurs in the same temperature range as for non-nitroxide polystyrene (400 °C). However the PS-T thermal degradation curve shows an additional step of mass loss at temperatures below 300 °C, suggesting two reactions, one apparently being the cleavage of the polystyrene–nitroxide bond followed by depolymerization, and the other being the breakage of the N-O bond in the TEMPO moiety, the importance of both reactions changing with increasing temperature.

The lack of knowledge of the position and nature of the initial scission of the polystyrene thermal degradation has restricted its quantitative analysis.

Taking into account this background, the goals of this work are twofold: (i) First, to define a process to achieve the thermal decomposition of conventional (free-radical) polystyrene in one step, and (ii) to compare the developed process for the thermal pyrolysis of conventional PS with another in which PS possessing a nitroxide end-functionality is used. This functionality is introduced in the polymer previously polymerizing styrene in the presence of the TEMPO nitroxide (PS-T) (TEMPO is (2,2,6,6-tetramethylpiperidin-1-yl) oxyl). For the comparison, precise pyrolysis conditions to induce depolymerization reactions that generate styrene monomer as main product and chemicals of high energetic value in the absence of solvents and catalysts at relatively mild conditions of temperature and pressure are first determined. TEMPO is used to provide living character to the free radical polymerization producing polystyrene with an extreme ended in a nitroxide moiety (PS-T) that, from the origin, has characteristics that favor depolymerization. As mentioned above, the hypothesis behind this work is that PS-T will depolymerize in a certain range of temperatures (via unzipping) by chain-end initiation of the reaction at the nitroxide functionality, promoting depropagation reactions in relatively mild temperature conditions or moderately above the polystyrene ceiling temperature. It is believed that above the T_c of polystyrene the uncapping (activation) reaction of the nitroxide moiety at the end of the polystyrene chain will leave a polystyryl radical that will undergo unzipping. The experiments seem to validate this hypothesis to some extent. On the other hand, a mathematical model of the pyrolysis reaction is developed to explain major effects observed and especially the effect of the end-nitroxide group in the PS-T chain.

2. Materials and Methods

2.1. Materials

Styrene (99%) was purified using an inhibitor removal column (4-tert-butylcatechol). Benzoyl peroxide (98%), (2, 2, 6, 6-tetramethyl-1-piperidinyl-1-yl) oxyl (TEMPO), all reactants from Aldrich (St. Louis Missouri, USA) (Manufacturer name, city, state if US or Canada, country) and industrial grade methanol (90%) (Proquisa, Saltillo, Mexico) were used as received.

2.2. Reaction System

The depolymerization system used in this work is shown in Figure 2 and consists of a batch pressurized reactor and a condenser.

The 50 mL reactor vase is made of stainless steel, and it comprises a heating source in the form of an electric mantle which provides homogeneous temperature increase inside the reactor and keeps the reaction temperature between 300 and 500 °C with the help of a thermocouple situated inside the reaction mixture and a digital controller that manipulates the current sent to the heating mantle. The reactor is also fitted with a manometer, inlet and outlet valves (to feed inert gas to the system and generate a free oxygen atmosphere), and a third outlet valve that connects the reactor to a double tube condenser which uses a low temperature fluid (−5 °C) that allows the rapid condensation of the generated vapors.

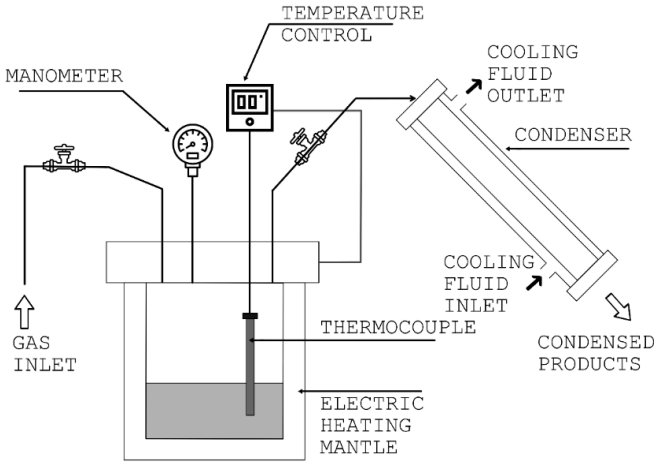

Figure 2. Depolymerization reaction system.

2.3. Polystyrene Synthesis Methods

Polystyrene that would be subjected to the pyrolysis experiments was synthesized by two different methods: by conventional free radical polymerization, and by nitroxide mediated radical polymerization (NMP).

In the conventional free radical polymerization (FRP), the reaction was performed in a batch bulk process at constant temperature (90 °C) in a 150 mL glass reactor, inert atmosphere, and continuous agitation, using benzoyl peroxide as initiator. The agitation was implemented via a mechanical agitator that was used until the viscosity of the reaction media made it not possible to continue in this way. After this point, reached at conversions above 80%, the reaction was left without agitation until conversions of 99% were reached and then stopped by lowering the reaction temperature to ambient temperature. The polymer was subsequently recovered by adding acetone to it (around 10–15% wt. with respect to the total mass of polymer) to allow the material to flow, followed by precipitation of the reaction mixture in methanol. The precipitate was later filtered and dried, obtaining white polymer dust as product.

Styrene polymerizations by the NMP method were performed using BPO as initiator and TEMPO as the stable free radical, varying the nitroxide (N) to initiator (I) ratio; three levels were established (N/I: 1.3, 1.1, and 0.9), they were all performed in a batch reactor at constant temperature (130 °C) with continuous agitation and under inert atmosphere. When conversions of 99% were reached, the reactions were stopped by submerging the reactor in a cooling ice bath, lowering the system temperature. The polymer from the reaction mixture was recovered following the same procedure described before for the PS produced by conventional FRP. The product was obtained as a white dust.

The polymers obtained by FRP and NMP were analyzed by size exclusion chromatography (SEC) using an Agilent Technologies Mod G7810A chromatograph (Agilent Technologies, Santa Clara, CA, USA) at 40 °C, with a sample concentration of 1 mg mL^{-1}, solvent flow of 1 mL/min and a polystyrene standard (Agilent Technologies, Santa Clara, CA, USA); the results are summarized in Table 1. The experiments were designed to obtain approximately the same number average molecular weight in all the cases (40–50,000 Da).

Table 1. Properties of synthesized polystyrene.

Sample	M_n	M_w	M_w/M_n
NMP, N/I = 1.3	46,100	56,800	1.23
NMP, N/I = 1.1	44,800	56,900	1.27
NMP, N/I = 0.9	42,500	55,500	1.3
FRP	50,040	96,700	1.9

2.4. Polystyrene Thermal Pyrolysis Experiments

The process to depolymerize all the polystyrene samples was the same and started by introducing 10 g of the synthesized plastic material inside the reactor and displacing the oxygen atmosphere with nitrogen to guarantee that the experiment was developed under inert conditions. Once this was achieved, all the valves of the reactor were closed and the temperature was rapidly increased, provoking a pressure rise; the time needed to reach the defined temperature set point was between 5 to 7 min. When the pressure reached from 7 to 12 psig, the valve connecting the reactor to the condenser was turned open, allowing the vapor products to migrate from the reactor to the condenser, after which the products were recovered as a liquid mixture. After reaching the temperature set point, the reaction proceeded until the liquid product was no longer obtained (about 10 min). The total reaction time was considered from the point at which the heating started to the moment at which the liquid outflow stopped. Experiments were carried out varying the pyrolysis temperature: 390, 420, and 450 °C and the source polystyrene (see Table 2), to investigate the effect of this variable on the prepared samples. After the reaction was finished and the reactor was cooled, two types of samples were obtained from each experiment: a liquid mixture from the condensed vapors and the residue left in the reactor in the form of a dark-colored oil with some solid degradation fragments (in the following discussion this will be referred as the solid fraction). Only the condensed liquid mixture was analyzed since it contains the most valuable products (including the monomer).

Table 2. Pyrolysis experiments performed.

Sample	Pyrolysis Temperature		
NMP, N/I = 1.3	390 °C * (Tri)	420 °C (Tri)	450 °C (Tri)
NMP, N/I = 1.1	390 °C	420 °C	450 °C
NMP, N/I = 0.9	390 °C	420 °C	450 °C
FRP	390 °C (Tri)	420 °C (Tri)	450 °C (Tri)

* (Tri) = Run and analyzed by triplicate.

3. Results

3.1. Product Analysis

The obtained products from the polystyrene pyrolysis experiments were analyzed to determine the most abundant components present in the liquid mixture. A gas chromatograph (Thermo Finnigan by Thermo Fisher Scientific Waltham, MA, USA) equipped with a selective mass detector (DSQ Trace 2000) (Thermo Electron Corporation, Austin, TX, USA) and a Thermo TG-5ms column were used. All the samples were analyzed under the same conditions with helium as the carrier gas. The temperature program was as follows: the temperature was held at 60 °C for 3 min, then programmed to reach 300 °C at a heating rate of 10 °C min^{-1} and held at that temperature for 10 min. The injector temperature was set at 250 °C. The transfer temperature line of the mass detector was set at 280 °C and the mass range was from 32 to 650 amu. The products were identified according to their fragmentation patterns using a library included in the software of the chromatograph.

3.2. Kinetic Model

As described before, the radical process of conventional polystyrene pyrolysis comprises the typical steps of initiation, propagation, transfer to polymer, and termination: Although initiation can occur due to several causes, there seems to be general agreement that consists of the formation of free radicals after bond breakage by the action of heat mainly either at a chain-end (which results in the production of monomer) or at a mid-chain position along the polymer backbone. Propagation covers the competition of three different reaction mechanisms: unzipping, intramolecular, and intermolecular hydrogen transfer, the first one is sometimes also called depolymerization and is taken to be the reverse

of chain growth, while transfer to polymer consists in the abstraction of a hydrogen from the same or another molecule. The termination step can occur via recombination and disproportionation reactions.

Our proposed model, which aims to describe both conventional and nitroxide-modified polystyrene pyrolysis behavior, contains the following reactions: mid-chain random scission, end chain scission or activation, transfer to polymer, β-scission, depropagation, and termination by combination and by disproportionation, as can be seen in Table 3. P_n denotes living polymer with length n, while R_n, S_n, D_n, M, and $M\cdot$ denote live polymer of length n with nitroxide in one end, dormant polymer of length n, dead polymer of length n, monomer and monomer radical, respectively. The kinetic constants are denoted as: k_b (mid-chain random scission), k_{be} (end-chain scission), $k_{tr\beta}$ (transfer to polymer + β-scission, simplified mechanism), k_{rev} (depropagation), k_{tc} (termination by combination), and k_{td} (termination by disproportionation). To simplify the description, some assumptions and approximations are made:

Table 3. Polystyrene depolymerization kinetic mechanism including the presence of nitroxide-end polystyrene.

Mechanism	Reaction
Mid chain random scission, dormant polymer	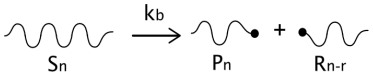
Mid chain random scission, dead polymer	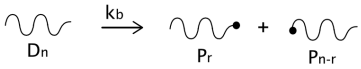
End chain scission, dead polymer	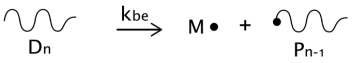
* End chain scission or activation, dormant polymer	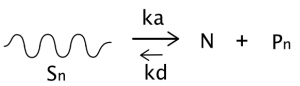
Transfer to polymer + β-scission (1)	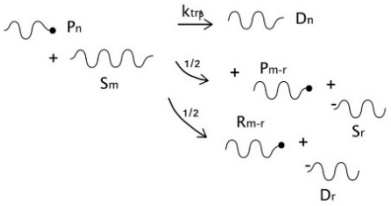
Transfer to polymer + β-scission (2)	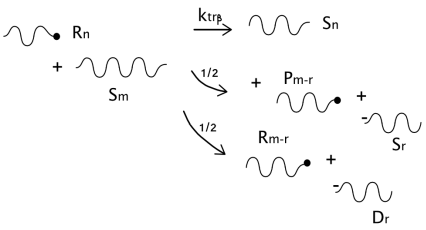
Transfer to polymer + β-scission (3)	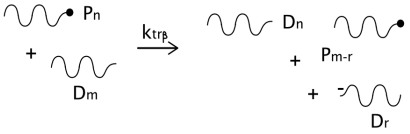

Table 3. *Cont.*

Mechanism	Reaction
Transfer to polymer + β-scission (4)	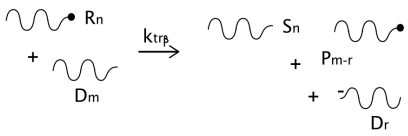
De-propagation	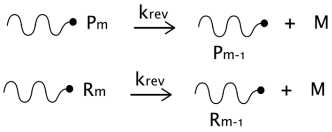
Termination by combination	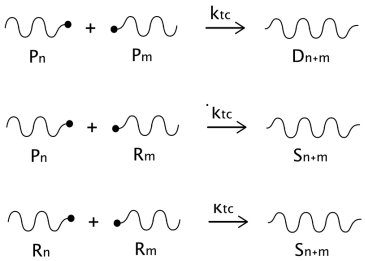
Termination by disproportionation	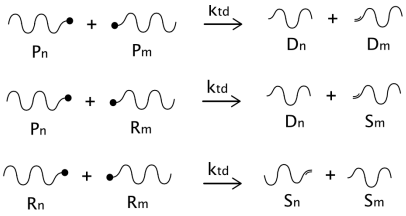
Termination with monomeric radicals	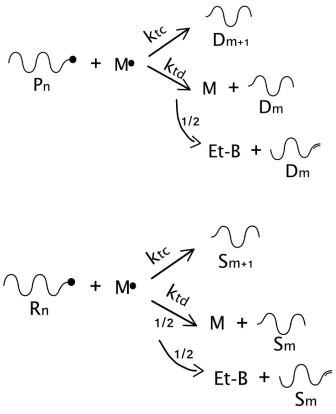

* Notice that this is the same reaction illustrated in Figure 2.

Dormant polymer with one or two nitroxide-functionalized ends will be lumped together into a single quantity. Upon mid-chain random scission of these species to form two radicals, it will be assumed that only one radical contains a nitroxide-functionalized end. Notice that as the number of chain ends increases in the system due to the pyrolysis process, the probability of a chain ending in a nitroxide moiety decreases. This introduces some error, but it will be neglected for simplicity since it is assumed that on the average the error introduced is small.

Initiation includes the possible formation of free radicals either in the terminal or in a mid-chain random position. The corresponding kinetic coefficients could be different depending on the position (end-chain or mid-chain) since the radicals produced in each case are of different nature, mid-chain

scission forms one primary radical and one secondary benzyl radical, while end-chain scission forms a secondary benzyl radical; both reactions can occur on dormant or dead polymer (S_n, D_n) as described in Table 3. Transfer to polymer followed by β-scission can occur between any of two types of living chains (normal, P_n, or with a nitroxide-end functionality, R_n) and one of two types of inactive chains (dormant, S_n, or dead, D_n). In the case of dormant polymer, the initiation can also occur at the nitroxide end via the activation reaction. The rest of the reactions, depropagation and termination, are the same as those appearing in the standard mechanism of free-radical polymerization, with subtle variations depending on the possible presence of a nitroxide-end functionality in one or both reacting chains.

3.3. Mathematical Model

Based on the described reaction scheme, the corresponding mathematical model was formulated writing a mass balance equation for each species. Then, the method of moments was used to keep track of changes of the average molecular weights as a function of time.

Dead polymer, $n = 1, \ldots, \infty$

$$\begin{aligned}\frac{dD_n}{dt} = -k_b n D_n \quad & -k_{be} D_n + k_{tr\beta} P_n \sum_{m=1}^{\infty} m\, D_m - k_{tr\beta}\, n\, D_n \sum_{m=1}^{\infty} P_m \\ & + k_{tr\beta}\left(\sum_{s=1}^{\infty} P_s\right) \sum_{m=n+1}^{\infty} m\, D_m\left(\tfrac{1}{m}\right) + k_{tr\beta} P_n \sum_{m=1}^{\infty} m\, S_m \\ & + \tfrac{k_{tr\beta}}{2}\left(\sum_{r=1}^{\infty} P_r\right) \sum_{m=n+1}^{\infty} m\, S_m\left(\tfrac{1}{m}\right) + \tfrac{k_{tr\beta}}{2}\left(\sum_{r=1}^{\infty} R_r\right) \sum_{m=n+1}^{\infty} m\, S_m\left(\tfrac{1}{m}\right) \\ & + k_{tr\beta}\left(\sum_{r=1}^{\infty} R_r\right) \sum_{m=n+1}^{\infty} m\, D_m\left(\tfrac{1}{m}\right) - k_{tr\beta}\, n D_n \sum_{m=1}^{\infty} R_m \\ & + \tfrac{k_{tc}}{2} \sum_{m=1}^{n-1} P_m P_{n-m} + k_{td} P_n \sum_{m=1}^{\infty} P_m + k_{td} P_n \sum_{m=1}^{\infty} R_m + k_{tc} P_{n-1}\, M \\ & + k_{td} P_n\, M\end{aligned} \tag{1}$$

Dormant polymer, $n = 1, \ldots, \infty$

$$\begin{aligned}\frac{dS_n}{dt} = -k_b n S_n \quad & -k_a S_n + k_d M\, P_n - k_{tr\beta}\, n\, S_n \sum_{m=1}^{\infty} P_m + \tfrac{k_{tr\beta}}{2}\left(\sum_{r=1}^{\infty} P_r\right) \sum_{m=n+1}^{\infty} m\, S_m\left(\tfrac{1}{m}\right) \\ & - k_{tr\beta}\, n\, S_n \sum_{m=1}^{\infty} R_m + k_{tr\beta}\, R_n \sum_{m=1}^{\infty} m\, S_m \\ & + \tfrac{k_{tr\beta}}{2}\left(\sum_{r=1}^{\infty} R_r\right) \sum_{m=n+1}^{\infty} m\, S_m\left(\tfrac{1}{m}\right) + k_{tr\beta} R_n \sum_{m=1}^{\infty} m\, D_m \\ & + \tfrac{1}{2} k_{tc} \sum_{m=1}^{n-1} P_m R_{n-m} + \tfrac{1}{2} k_{tc} \sum_{m=1}^{n-1} R_m R_{n-m} + k_{td} R_n \sum_{m=1}^{\infty} P_m \\ & + k_{td} R_n \sum_{m=1}^{\infty} R_m + k_{tc} R_{n-1} M\cdot + k_{td} R_n M\end{aligned} \tag{2}$$

Live polymer, $n = 1, \ldots, \infty$

$$\begin{aligned}\frac{dP_n}{dt} = k_a S_n - k_d N P_n \quad & +2k_b \sum_{m=n+1}^{\infty} m\, D_m\left(\tfrac{1}{m}\right) + k_{be} D_{n+1} + k_b \sum_{m=n+1}^{\infty} m\, S_m\left(\tfrac{1}{m}\right) \\ & - k_{rev} P_n + k_{rev} P_{n+1} - k_{tr\beta} P_n \sum_{m=1}^{\infty} m\, S_m \\ & + \tfrac{k_{tr\beta}}{2}\left(\sum_{r=1}^{\infty} P_r\right) \sum_{m=n+1}^{\infty} m\, S_m\left(\tfrac{1}{m}\right) + \tfrac{k_{tr\beta}}{2}\left(\sum_{r=1}^{\infty} R_r\right) \sum_{m=n+1}^{\infty} m\, S_m\left(\tfrac{1}{m}\right) \\ & - k_{tr\beta} P_n \sum_{m=n+1}^{\infty} m\, D_m + k_{tr\beta} \sum_{r=1}^{\infty} P_r \sum_{m=1}^{\infty} m\, D_m\left(\tfrac{1}{m}\right) \\ & + k_{tr\beta} \sum_{r=1}^{\infty} R_r \sum_{m=n+1}^{\infty} m\, D_m\left(\tfrac{1}{m}\right) - k_t P_n \sum_{m=1}^{\infty} P_m - k_t P_n \sum_{m=1}^{\infty} R_m - k_t P_n M\end{aligned} \tag{3}$$

Live polymer with a nitroxide at the chain-end, $n = 1, \ldots, \infty$

$$\begin{aligned}\frac{dR_n}{dt} = k_b \sum_{m=n+1}^{\infty} & m\, S_m\left(\tfrac{1}{m}\right) + \frac{k_{tr\beta}}{2}\left(\sum_{m=1}^{\infty} P_m\right)\sum_{r=n+1}^{\infty} r\, S_r\left(\tfrac{1}{r}\right) - k_{tr\beta}R_n \sum_{m=1}^{\infty} m\, S_m \\ & + \frac{k_{tr\beta}}{2}\left(\sum_{r=1}^{\infty} R_r\right)\sum_{m=n+1}^{\infty} m\, S_m\left(\tfrac{1}{m}\right) - k_{tr\beta}R_n \sum_{m=1}^{\infty} m\, D_m + k_{rev}R_{n+1} \\ & - k_{rev}R_n - k_t R_n \sum_{m=1}^{\infty} P_m - k_t R_n \sum_{m=1}^{\infty} R_m - k_t R_n M\end{aligned} \tag{4}$$

Monomer

$$\frac{dM}{dt} = k_{rev}\sum_{m=1}^{\infty} P_m + \frac{1}{2}k_{td}M\cdot\sum_{m=1}^{\infty} P_m + k_{rev}\sum_{m=1}^{\infty} R_m + \frac{1}{2}k_{td}M\cdot\sum_{m=1}^{\infty} R_m \tag{5}$$

Monomeric radicals

$$\frac{dM}{dt} = k_{rev}\sum_{m=1}^{\infty} P_m + \frac{1}{2}k_{td}M\cdot\sum_{m=1}^{\infty} P_m + k_{rev}\sum_{m=1}^{\infty} R_m + \frac{1}{2}k_{td}M\cdot\sum_{m=1}^{\infty} R_m \tag{6}$$

Nitroxide radicals

$$\frac{dN}{dt} = k_a S_n - k_d\, N\cdot P_n \tag{7}$$

Ethyl benzene

$$\frac{dEt-B}{dt} = \frac{1}{2}k_{td}M\cdot\sum_{m=1}^{\infty} P_m + \frac{1}{2}k_{td}M\cdot\sum_{m=1}^{\infty} R_m \tag{8}$$

Four polymer populations exist in this system: Dead polymer, dormant polymer, growing polymeric radical and polymer radical with a nitroxide end functionality; moments for these species are defined in Equations (9)–(12) respectively:

$$\lambda_i = \sum_r r^i D_r \tag{9}$$

$$\xi_i = \sum_r r^i S_r \tag{10}$$

$$\mu_i = \sum_r r^i P_r \tag{11}$$

$$\psi_i = \sum_r r^i R_r \tag{12}$$

The method of moments applied to the previously described balance equations generates Equations (13)–(15) for the zero-th, first, and second moments of dead polymer, respectively, Equations (16)–(18) for the moments of dormant polymer, Equations (19)–(21) for polymeric radical moments, and Equations (22)–(24) for the moments of polymeric radicals with a nitroxide end functionality.

$$\begin{aligned}\frac{d\lambda_0}{dt} = \; & -k_b\lambda_1 - k_{be}\lambda_0 + k_{td}{\mu_0}^2 + \tfrac{k_{tc}}{2}{\mu_0}^2 + k_{td}\mu_0\psi_0 + k_{tc}M\cdot\mu_0 + k_{td}M\cdot\mu_0 \\ & + k_{tr\beta}\mu_0\lambda_1 - k_{tr\beta}\mu_0\lambda_1 + k_{tr\beta}(\lambda_1-\lambda_0)(\mu_0+\psi_0) + k_{tr\beta}\mu_0\xi_1 \\ & + \tfrac{k_{tr\beta}}{2}(\mu_0+\psi_0)B_0(\xi_1-\xi_0) - k_{tr\beta}\lambda_1\psi_0 \\ & B_0 = 1\end{aligned} \tag{13}$$

$$\begin{aligned}\frac{d\lambda_1}{dt} = -k_b\lambda_2 - \; & k_{be}\lambda_1 + k_{td}\mu_1\mu_0 + k_{tc}\mu_1\mu_0 + k_{td}\mu_1\psi_0 + k_{tc}M\,(\mu_1+\mu_0) + k_{td}M\cdot\mu_1 \\ & + k_{tr\beta}[\mu_1\lambda_1 - \lambda_2\mu_0 + \tfrac{(\mu_0+\psi_0)}{2}(\lambda_2-\lambda_1) + \mu_1\xi_1 \\ & + \tfrac{1}{4}(\mu_0+\psi_0)(\xi_2-\xi_1) - \lambda_2\psi_0]\end{aligned} \tag{14}$$

$$\frac{d\lambda_2}{dt} = -k_b\lambda_3 - \begin{aligned} & k_{be}\lambda_2 + k_{td}\mu_2\mu_0 + k_{tc}\left(\mu_0\mu_2 + {\mu_1}^2\right) + k_{td}\mu_2\psi_0 + k_{tc}M\cdot(\mu_2 + 2\mu_1 \\ & +\mu_0) + k_{td}M\cdot\mu_2 + k_{tr\beta}[\mu_2\lambda_1 - \lambda_3\mu_0 \\ & +(\mu_0 + \psi_0)\left(\tfrac{1}{3}\lambda_3 - \tfrac{1}{2}\lambda_2 + \tfrac{1}{6}\lambda_1\right) + \mu_2\xi_1 \\ & +\tfrac{1}{2}(\mu_0 + \psi_0)\left(\tfrac{1}{3}\xi_3 - \tfrac{1}{2}\xi_2 + \tfrac{1}{6}\xi_1\right) - \lambda_3\psi_0] \end{aligned} \quad (15)$$

$$\frac{d\xi_0}{dt} = -k_b\xi_1 - \begin{aligned} & k_a\xi_0 + k_dN\mu_0 + \tfrac{k_{tc}}{2}(\mu_0\psi_0 + \psi_0\psi_0) + k_{td}(\psi_0\mu_0) + k_{td}{\psi_0}^2 + k_{tc}M \\ & \cdot\psi_0 + k_{td}\psi_0M\cdot - k_{tr\beta}\xi_1\mu_0 - k_{tr\beta}\xi_1\psi_0 + \tfrac{k_{tr\beta}}{2}(\mu_0 + \psi_0)(\xi_1 - \xi_0) \\ & +k_{tr\beta}\psi_0(\xi_1 + \lambda_1) \end{aligned} \quad (16)$$

$$\frac{d\xi_1}{dt} = -k_b\xi_2 - \begin{aligned} & k_a\xi_1 + k_dN\mu_1 + \tfrac{k_{tc}}{2}(\mu_1\psi_0 + \mu_0\psi_1) + k_{tc}\psi_1\psi_0 + k_{td}(\psi_1\mu_0) \\ & +k_{td}\psi_1\psi_0 + k_{tc}M\cdot(\psi_0 + \psi_1) + k_{td}\psi_1M - k_{tr\beta}\xi_2\mu_0 - k_{tr\beta}\xi_2\psi_0 \\ & +\tfrac{k_{tr\beta}}{4}(\mu_0 + \psi_0)(\xi_2 - \xi_1) + k_{tr\beta}\psi_1(\xi_1 + \lambda_1) \end{aligned} \quad (17)$$

$$\frac{d\xi_2}{dt} = -k_b\xi_3 - \begin{aligned} & k_a\xi_2 + k_dN\mu_2 + \tfrac{k_{tc}}{2}(\mu_2\psi_0 + 2\mu_1\psi_1 + \mu_0\psi_2) + k_{tc}\left(\psi_2\psi_0 + {\psi_1}^2\right) \\ & +k_{td}(\psi_2\mu_0) + k_{td}\psi_2\psi_0 + k_{tc}M\,(\psi_2 + 2\psi_1 + \psi_0) + k_{td}\psi_2M \\ & -k_{tr\beta}\xi_3\mu_0 - k_{tr\beta}\xi_3\psi_0 + \tfrac{k_{tr\beta}}{2}(\mu_0 + \psi_0)\left(\tfrac{1}{3}\xi_3 - \tfrac{1}{2}\xi_2 + \tfrac{1}{6}\xi_1\right) \\ & +k_{tr\beta}\psi_2(\xi_1 + \lambda_1) \end{aligned} \quad (18)$$

$$\frac{d\mu_0}{dt} = k_a\xi_0 - k_dN\mu_0 \quad \begin{aligned} & +k_{be}\lambda_0 - k_t{\mu_0}^2 - k_t\mu_0\psi_0 - k_t\mu_0M - k_{tr\beta}\mu_0\xi_1 \\ & +k_{tr\beta}(\mu_0 + \psi_0)(\lambda_1 - \lambda_0) - k_{tr\beta}\mu_0\lambda_1 + \tfrac{1}{2}k_{tr\beta}(\mu_0 + \psi_0)(\xi_1 - \xi_0) \\ & +2k_b[(\lambda_1 - \lambda_0) + (\xi_1 - \xi_0)] \end{aligned} \quad (19)$$

$$\begin{aligned} & \frac{d\mu_1}{dt} = k_a\xi_1 - k_dN\,\mu_1 + k_{be}(\lambda_1 - \lambda_0) - k_{rev}\mu_1 + k_{rev}(\mu_1 - \mu_0) - k_t\mu_1\mu_0 - k_t\mu_1\psi_0 - k_t\mu_1M \\ & -k_{tr\beta}\mu_1\lambda_1 + k_{tr\beta}(\mu_0 + \psi_0)\left[\tfrac{1}{2}(\lambda_2 - \lambda_1)\right] - k_{tr\beta}\mu_1\xi_1 + \tfrac{1}{2}k_{tr\beta}(\mu_0 + \psi_0)\left[\tfrac{1}{2}(\xi_2 - \xi_1)\right] + k_b\left[(\lambda_2 - \lambda_1) + \tfrac{1}{2}(\xi_2 - \xi_1)\right] \end{aligned} \quad (20)$$

$$\frac{d\mu_2}{dt} = k_a\xi_2 - k_dN\mu_2 \quad \begin{aligned} & +k_{be}(\lambda_2 - 2\lambda_1 + \lambda_0) - k_{rev}\mu_2 + k_{rev}(\mu_2 - 2\mu_1 + \mu_0) - k_t\mu_2\mu_0 \\ & -k_t\mu_2\psi_0 - k_t\mu_2M - k_{tr\beta}\mu_2\lambda_1 + k_{tr\beta}(\mu_0 + \psi_0)\left[\tfrac{1}{3}\lambda_3 - \tfrac{1}{2}\lambda_2 + \tfrac{1}{6}\lambda_1\right] \\ & -k_{tr\beta}\mu_2\xi_1 + \tfrac{1}{2}k_{tr\beta}(\mu_0 + \psi_0)\left[\tfrac{1}{3}\xi_3 - \tfrac{1}{2}\xi_2 + \tfrac{1}{6}\xi_1\right] \\ & +2k_b\left[\tfrac{1}{3}\lambda_3 - \tfrac{1}{2}\lambda_2 + \tfrac{1}{6}\lambda_1 + \tfrac{1}{3}\xi_3 - \tfrac{1}{2}\xi_2 + \tfrac{1}{6}\xi_1\right] \end{aligned} \quad (21)$$

$$\frac{d\psi_0}{dt} = -k_t\psi_0\mu_0 \quad \begin{aligned} & -k_t{\psi_0}^2 - k_t\psi_0M + k_b(\xi_1 - \xi_0) + \tfrac{1}{2}k_{tr\beta}(\mu_0 + \psi_0)(\xi_1 - \xi_0) \\ & -k_{tr\beta}\psi_0(\xi_1 + \lambda_1) \end{aligned} \quad (22)$$

$$\frac{d\psi_1}{dt} = -k_{rev}\psi_0 \quad \begin{aligned} & -k_t\psi_1\mu_0 - k_t\psi_1\psi_0 - k_t\psi_1M + \tfrac{k_b}{2}(\xi_2 - \xi_1) \\ & +\tfrac{1}{2}k_{tr\beta}(\mu_0 + \psi_0)\left[\tfrac{1}{2}(\xi_2 - \xi_1)\right] - k_{tr\beta}\psi_1(\xi_1 + \lambda_1) \end{aligned} \quad (23)$$

$$\frac{d\psi_2}{dt} = k_{rev}(\psi_2 - \quad \begin{aligned} & 2\psi_1 + \psi_0) - k_{rev}\psi_2 - k_t\psi_2\mu_0 - k_t\psi_2\psi_0 - k_t\psi_2M \\ & +k_b\left[\tfrac{1}{3}\xi_3 - \tfrac{1}{2}\xi_2 + \tfrac{1}{6}\xi_1\right] + \tfrac{1}{2}k_{tr\beta}(\mu_0 + \psi_0)\left[\tfrac{1}{3}\xi_3 - \tfrac{1}{2}\xi_2 + \tfrac{1}{6}\xi_1\right] \\ & -k_{tr\beta}\psi_2(\xi_1 + \lambda_1) \end{aligned} \quad (24)$$

From the previous equations, the number average molecular weight can be calculated using Equation (25)

$$M_n = \frac{\lambda_1 + \xi_1 + \mu_1 + \psi_1}{\lambda_0 + \xi_0 + \mu_0 + \psi_0} \quad (25)$$

Notice that the moment equations are not closed since the second moment depends on the third moment. To solve this problem, the well-known expression of Saidel and Katz [35] is used to estimate the third moment in terms of the lower moments.

$$\lambda_3 = \frac{\lambda_2}{\lambda_0\lambda_1}\left(2\lambda_2\lambda_0 - \lambda_1^2\right) \quad (26)$$

The mathematical model formulation yielded a set of ordinary differential equations (ODE's) that were numerically solved using the FORTRAN programming language with the DDASSL routine for the integration of the equations. Kinetic rate constant values were estimated to match the recorded experimental data as explained below.

3.4. Experimental Results

Since the experiments at the extreme levels of N/I (0 and 1.3) were run by triplicate, it was possible to estimate a pooled variance (σ^2) for the relevant responses (one for each temperature), and therefore error bars of 1σ are included in most of the plots.

Figure 3 shows the relative yields of the solid, liquid, and gaseous fractions obtained in the pyrolysis experiments using a given N/I ratio or by FRP carried at different temperatures. It can be noted that at higher pyrolysis temperatures the liquid fraction has a tendency to increase while the gas and solid fractions diminish. Comparing all the samples, the ones corresponding to the N/I ratio of 1.3 exhibit the higher values of recovered liquid fraction, the maximum value reached being 88% at 420 °C, while the lowest values correspond to the FRP samples. These results point out to a favorable effect of the presence of the nitroxide moiety at the end of the polymer chains on the pyrolysis process; more will be discussed below. All the percentages are referred to the total amount of polymer charged at the beginning of the experiments.

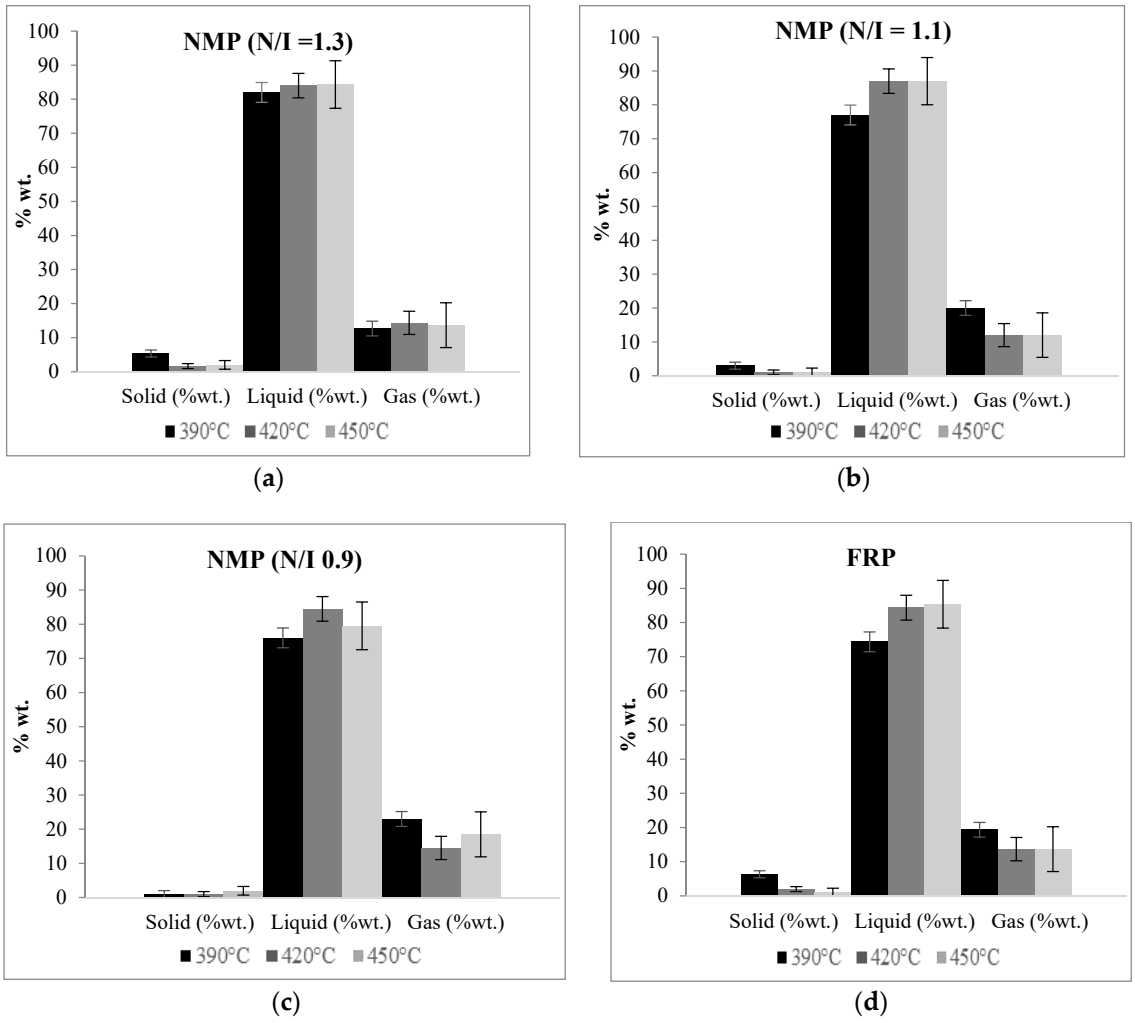

Figure 3. Yields of recovered fractions of the pyrolyzed samples: (**a**) N/I = 1.3, (**b**) N/I = 1.1, (**c**) N/I = 0.9, and (**d**) FRP.

Figure 4 shows the identified products of the PS pyrolysis in the liquid fraction; their relative amounts are plotted for each PS pyrolysis experiment at three reaction temperatures (390, 420, and 450 °C). The main product in all cases is styrene followed by styrene dimer in second place; an extra category is included denoted as "mixture", which corresponds to the sum of all the components that could not be identified, but individually amount to less than 1 wt.%. In the case of the FRP samples, stilbene and benzoic acid are also generated and the compounds in the non-identified mixture reach the highest values of all the samples.

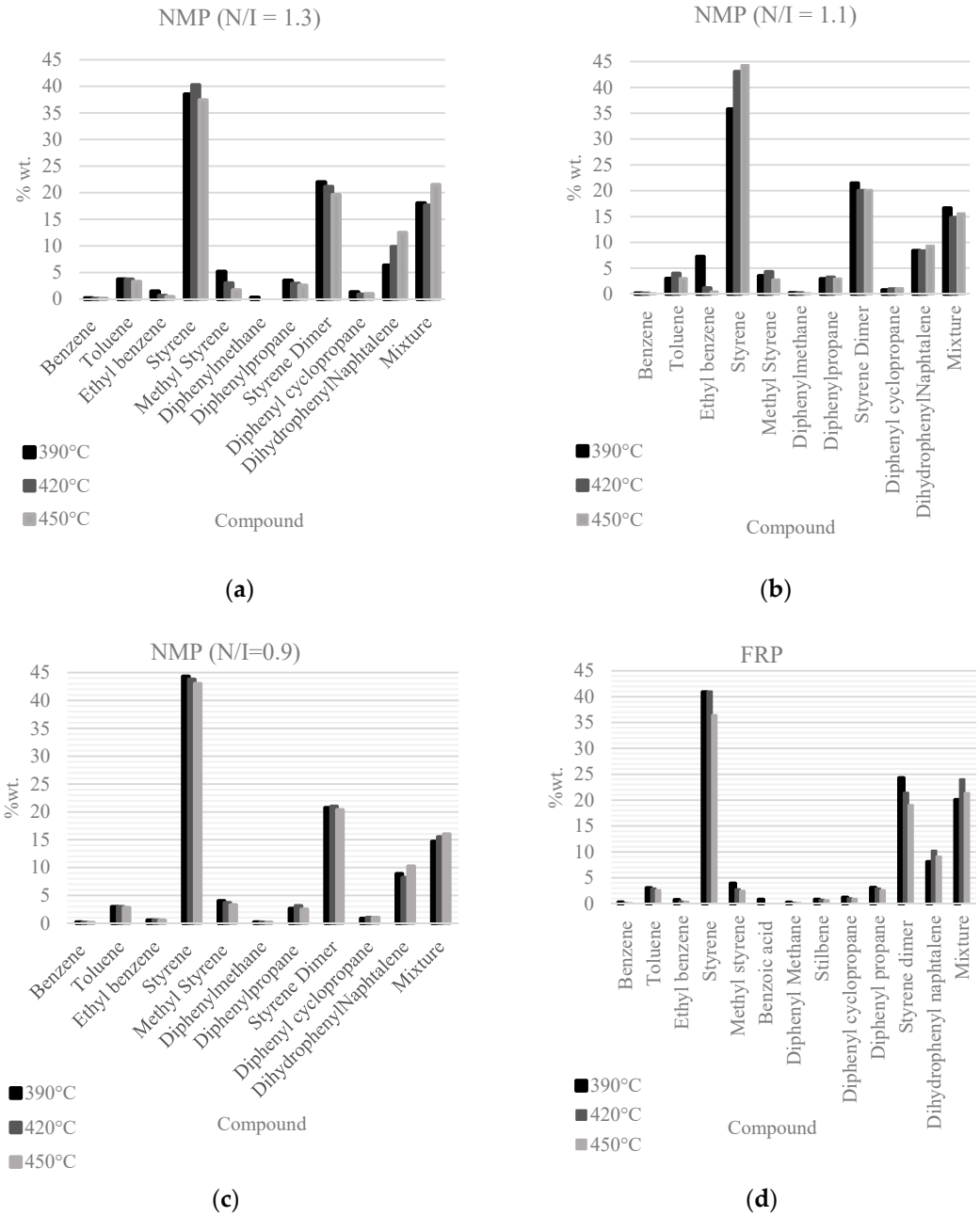

Figure 4. % wt. yield of the polystyrene depolymerization products in the liquid fraction: (**a**) N/I = 1.3, (**b**) N/I = 1.1, (**c**) N/I = 0.9, and (**d**) FRP.

Figure 5 shows the absolute yields of styrene monomer and styrene dimer of the different samples (with respect to the total load of PS, not only with respect to the liquid fraction recovered), indicating that at higher reaction temperatures the styrene dimer concentration tends to lower for the reaction

with N/I = 1.3, but it is the opposite for the reaction with N/I = 0.9. The monomer recovery yield exhibits a more complex behavior with temperature. For samples N/I = 1.1 and N/I = 0.9, the monomer recovery yield increases with higher temperatures, while for the N/I = 1.3 and the FRP samples maxima for monomer yield are exhibited. Clearly, not all the effects observed are significant, but in some cases the differences are evident, although generally moderate.

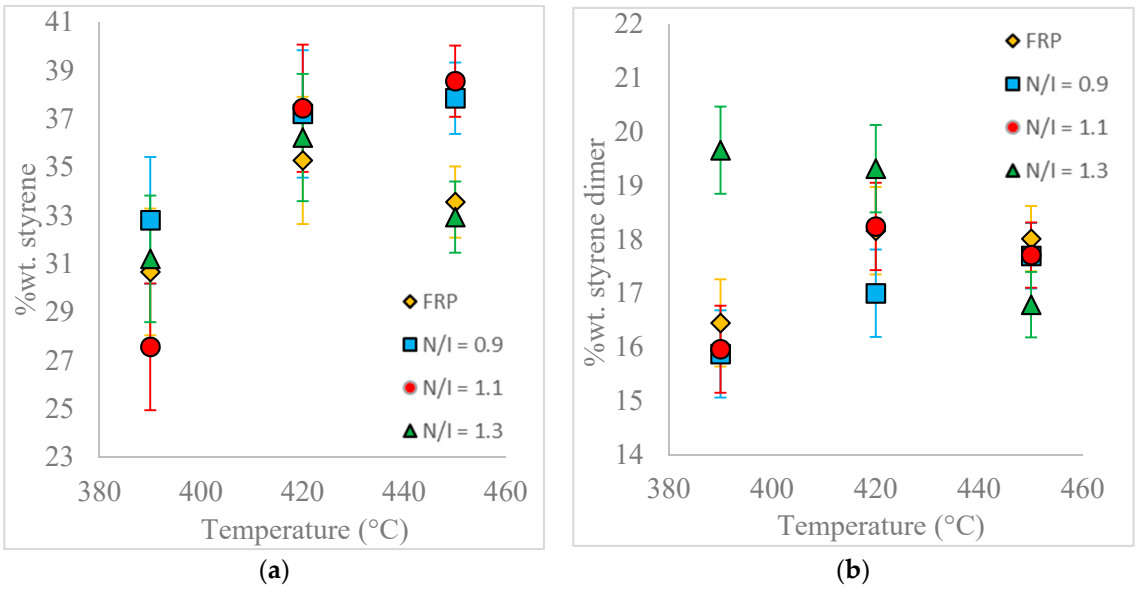

(**a**) (**b**)

Figure 5. Absolute yields of (**a**) styrene and (**b**) styrene dimer of the analyzed samples.

Comparing all the samples at 450 °C, the highest styrene yield (38.5%) is obtained using N/I = 1.1, and the lowest using N/I = 1.3 (around 33%) or, almost identical, FRP. Interestingly, at 420 °C all the samples with nitroxide show higher styrene yield than the FRP sample.

Pyrolysis reaction time is also affected by the use of PS samples containing nitroxide. Compared with FRP PS, the pyrolysis of these samples results in shorter reaction times at comparable temperatures, except in the case of FRP PS at 450 °C (Figure 6).

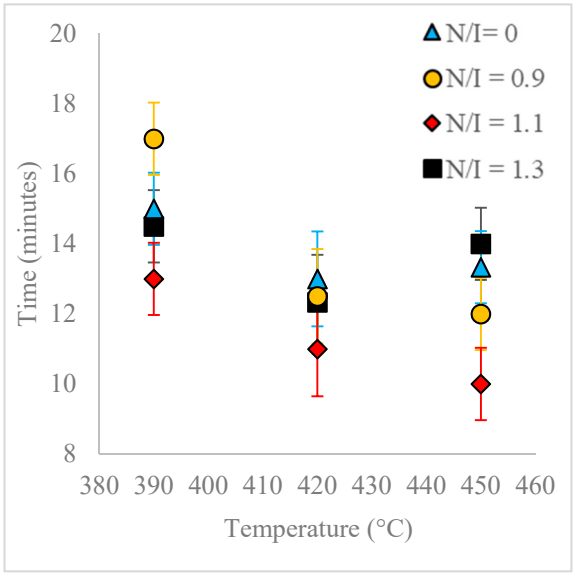

Figure 6. Reaction time (min) vs. temperature (C).

During the experimentation, special emphasis was put in obtaining reproducible results, and therefore the experimental design included replicate runs. Additionally, by performing replicate experiments, we were able to observe clear qualitative differences in the presence and absence of nitroxide in the samples. For example, for the blank reactions, the pressure increase was more abrupt, and the liquid recovery began in all cases at around 380 °C (during the temperature increase ramp). On the other hand, for the dormant polymer samples, especially those of N/I = 1.3, the pressure increase was smoother and more gradual, and the liquid recovery began before, at temperatures between 370–380 °C. These and other observations, as well as some of the quantitative results, reinforce the conclusion that the pyrolysis of PS samples with and without nitroxide ends behave differently.

3.5. Mathematical Modeling Results

The mathematical model developed here was intended as a first approach to qualitatively and quantitatively understand the experimental results observed. At this stage, only main experimental trends, particularly reaction time and the effect of nitroxide chain-ends on reaction time, were taken into account to tune the model parameters, since not much detailed information, such as time evolution of the molecular weight distribution or of the product distribution (in terms of individual chain-lengths), was available. Ongoing work in our group is directed towards getting more detailed experimental information as well as more detailed mathematical models.

With respect to the kinetic parameters, values are reported in the literature for some of them. Table 4 summarizes some rate constants for PS depolymerization available from the literature that were estimated in different reaction systems.

Table 4. Reaction kinetic constants of polystyrene depolymerization from literature sources.

Reference	**[36]**		**[37]**		**[38]**	
Processes	**A** [a,b]	**E** [b] **(kcal/mol)**	**A** [a,b]	**E** [b] **(kcal/mol)**	**A** [a,b]	**E** [b] **(kcal/mol)**
Chain fission $\left(s^{-1}\right)$	5.0×10^{13}	63.7	7.98×10^{15}	2.3	1.0×10^{16}	2.3
Chain fission allyl $\left(s^{-1}\right)$	5.0×10^{12}	58.6	-	-	5.5×10^{13}	2.3
H- abstraction of end chain $\left(\frac{L}{mol\ seg}\right)$	5.0×10^{7}	13.5	-	-	-	-
H-abstraction of mid chain $\left(\frac{L}{mol\ seg}\right)$	5×10^{7}	16.5	-	-	-	-
H-abstraction	-	-	1.5×10^{8}	13.3	2.1×10^{6}	12
Mid chain β-scission $\left(s^{-1}\right)$	1.2×10^{13}	27.0	2.62×10^{12}	12.9	4.1×10^{12}	11.4
End chain β-scission $\left(s^{-1}\right)$	1.6×10^{13}	25.8	2.62×10^{12}	12.9	4.1×10^{12}	11.4
Radical recombination $\left(\frac{L}{mol\ seg}\right)$	5.0×10^{6}	14.0	2.2×10^{9}	2.3	1.1×10^{11}	2.3
Disproportionation $\left(\frac{L}{mol\ seg}\right)$	-	-	1.14×10^{8}	2.3	5.5×10^{9}	2.3

[a] Units compatible with those shown in first column. [b] A and E are pre-exponential and activation energy in the corresponding Arrhenius expression for the kinetic constant.

Literature values for the kinetic constants were tested using the mathematical model in terms of moments described by the Equations (5)–(8) and (13)–(24); however, the sets of parameter values available in the literature were either incomplete or corresponded to kinetic models with differences with respect to the one proposed here. When they were tried in the present kinetic model, they yielded inconsistent results in the sense of high stiffness and/or non-convergence of the numerical integration of the differential equations, as well as some results without proper physical meaning.

4. Discussion

4.1. Sensitivity Analysis

Given the lack of useful values from the literature, it was decided to perform a sensitivity analysis to fit a consistent set of kinetic parameter values of the model. The results of the sensitivity analysis are summarized in Figures 7–11, which show essentially the sensitivity of the pyrolysis model in terms of

the evolution of the polymer M_n and the monomer generation with the time of reaction upon varying different reaction coefficients. The base set of used kinetic constants at 350 °C in all cases is listed in Table 5. In the value of M_n plotted the definition given by Equation (25) was used, which represents a lumped value of average molecular weight that includes all the present polymer populations (naturally, the terms corresponding to dormant polymer and live polymer with a nitroxide end are zero for the dead polymer case). The criterion used to choose the set of parameters of Table 5, among other viable sets, was that they produced qualitative results that were consistent with the experimental observations and also that their values fell in the vicinity of similar parameters reported in the literature when available (same order of magnitude). Clearly, the proper selection of kinetic parameters for this system is a difficult and still unsolved problem which requires further investigation. Ideally, the kinetic parameters should be evaluated by independent experiments as model-free as possible; however, this goal is quite challenging for systems exhibiting the complexity of the present one. The proposed kinetic parameters are assumed as a good starting point for further research, and are valuable to show the feasibility of the mathematical model presented and for parameter sensitivity studies, but it is important to mention that this parameter set is not unique and there may be other sets of values similarly viable and consistent with the experimental observations.

The discussion of Figures 6–11 is done by groups of plots. In each case analyzed, four plots are presented in each figure: two of them correspond to pyrolysis experiments of dead polymer having no functionality; the other two correspond to the pyrolysis of dormant polymer with a nitroxide functionality at its end. In the first two plots, the evolution (degradation) of M_n of the dead polymer and of the dormant polymer respectively is shown; in the other two plots, the evolution of monomer for the dead and dormant polymer is respectively exhibited.

Table 5. Depolymerization kinetic constants at 350 °C.

Mechanism (L $mol^{-1}s^{-1}$ Unless Indicated)	Variable	Value
End Chain scission (s^{-1})	k_{be}	8.0×10^2
Transfer + β-scission	k_{trb}	1.1×10^2
Depropagation (s^{-1})	k_{rev}	1.1×10^{-1}
Termination by combination	k_{tc}	5.8×10^1
Termination by disproportionation	k_{td}	2×10^1
Mid chain scission (s^{-1})	k_b	1.5×10^{-1}
Deactivation of dormant species (at 130 °C)	k_d	4.78×10^7 *
Activation of dormant species (s^{-1}) (at 130 °C)	k_a	3.16×10^{-3} *

* Arrhenius expressions: $k_d = 5 \times 10^9 \exp\left(-\frac{16{,}000}{RT}\right)$; $k_a = 4 \times 10^{13} \exp\left(-\frac{124{,}000}{RT}\right)$; R in J $mol^{-1}K^{-1}$ [39].

Figure 7 shows the effect of the variation of the value of k_{be} (end-chain scission) on the pyrolysis of dead and dormant polymer. Unexpectedly, in both cases, a smaller value of this kinetic coefficient results in a faster decomposition rate and in lower M_n at the end of the reaction time. In the following discussion the case of dead polymer will be taken as an illustration for the explanation, but the case of dormant polymer follows a similar pattern. To understand why this behavior is observed, the evolution of moments 0 and 1 of live and dead polymer were investigated and it was found that almost instantaneously most of the dead chains are activated; that is, they go from a dead state to live polymer (produced by the different available initiation mechanisms). There are however differences in the dynamics of this activation depending on the values of k_{be}. When lower values of this constant are used, the live polymer concentration rises more slowly (and the dead polymer concentration also decreases more slowly), but it reaches a higher maximum and then a higher stationary value, at the same time that the dead polymer concentration is less depleted in this case (higher stationary concentration). In fact, higher remaining concentration of dead polymer in these conditions favors a relatively faster steady formation of live polymer (via chain-end activation) and leads to a higher quasi-stationary concentration of live polymer (roughly proportional to $\mu_0 \approx \left[\frac{k_{be}\lambda_0}{k_t}\right]^{1/2}$, the lower value of k_{be} is more than compensated by a higher λ_0). Finally, an ultimate higher concentration of live polymer leads to

faster depropagation and higher monomer production. The effect of k_{be} is more pronounced for the pyrolysis of dead polymer than for dormant polymer. This is expected since a large portion of the initial decomposition step of the dormant polymer should occur at the nitroxide end, making the other contribution less important.

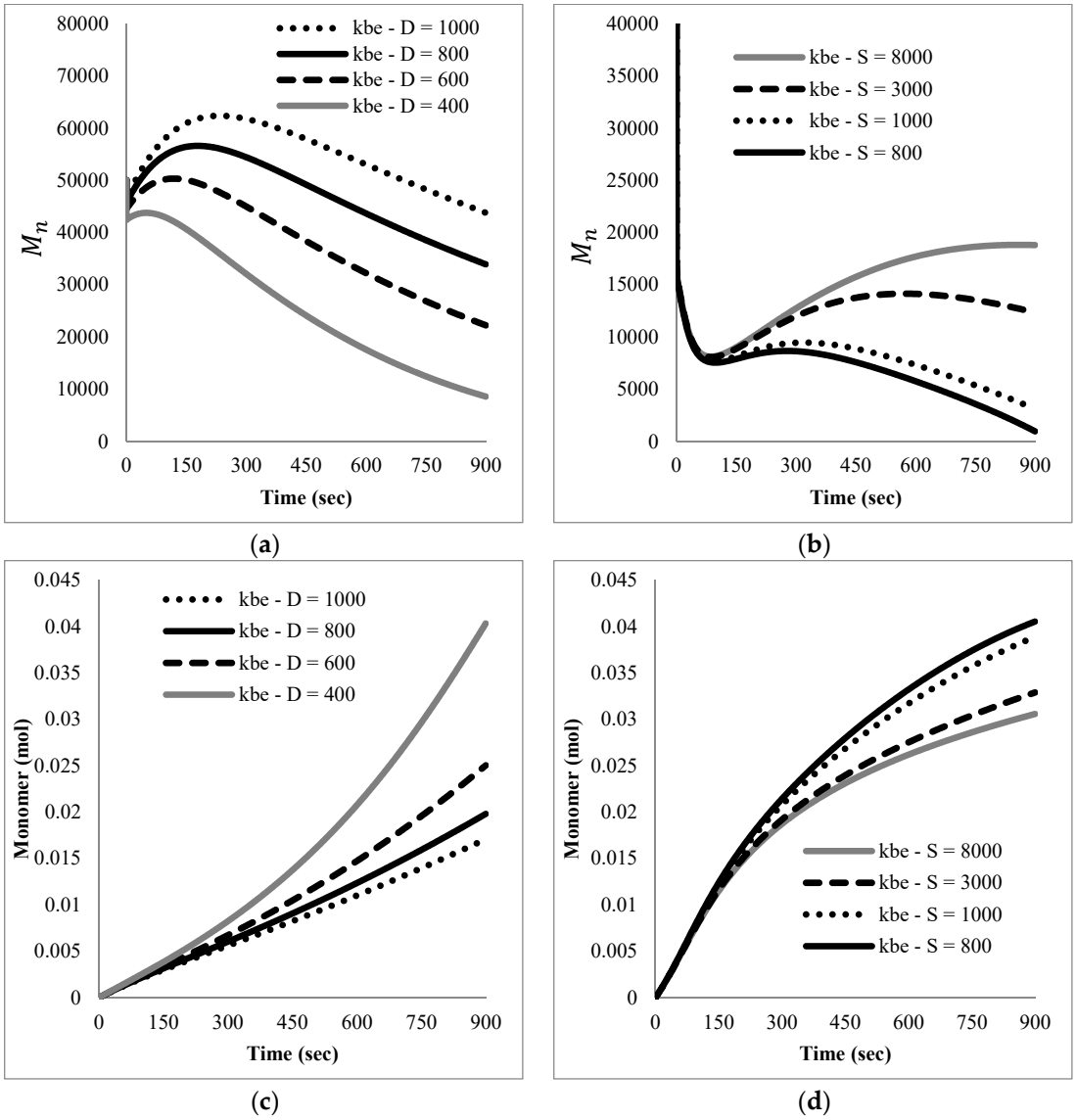

Figure 7. Effect of the variation of the chain-end scission coefficient, k_{be}, value on the pyrolysis M_n evolution of (**a**) dead polymer and (**b**) dormant polymer, and on the monomer generation of (**c**) dead polymer and (**d**) dormant polymer.

Figure 8 shows the sensitivity of the M_n evolution when the value of the transfer to polymer + β-scission coefficient, k_{trb}, is changed. As this value increases, the polymer decomposes faster, but the behavior shows significant quantitative differences for the dead and the dormant polymer. In both cases the value of M_n goes through a minimum, then increases to reach a maximum and finally steadily decreases; however, for the dormant polymer cases the initial minima are much more pronounced and the subsequent maxima are less marked, indicating a more effective decomposition in the case of dormant polymer. This is confirmed by the plots of monomer evolution that grows faster and reaches higher values (roughly double) for the case of dormant polymer pyrolysis compared to that of dead polymer.

Figure 9 shows the effect of the termination by combination value (k_{tc}) over the M_n evolution. For dead polymer the effect is quite complex. At early stages of the reaction (less than 100 s) M_n values reach a maximum, which is higher and is reached faster for higher values of k_{tc} (an expected output); however, as the activation reactions proceed, the faster dynamics apparently promoted by higher values of k_{tc} accelerate the polymer degradation leading faster to lower values of M_n. These shorter chains imply larger number of dead chain-ends that can undergo end-scission, accelerating the degradation of the polymer and the monomer production. Similar effects are present in the case of dormant polymer, but they are significantly attenuated by the competing mechanism of deactivation/degradation at the nitroxide end, which tends to dominate, especially at lower values of k_{tc}.

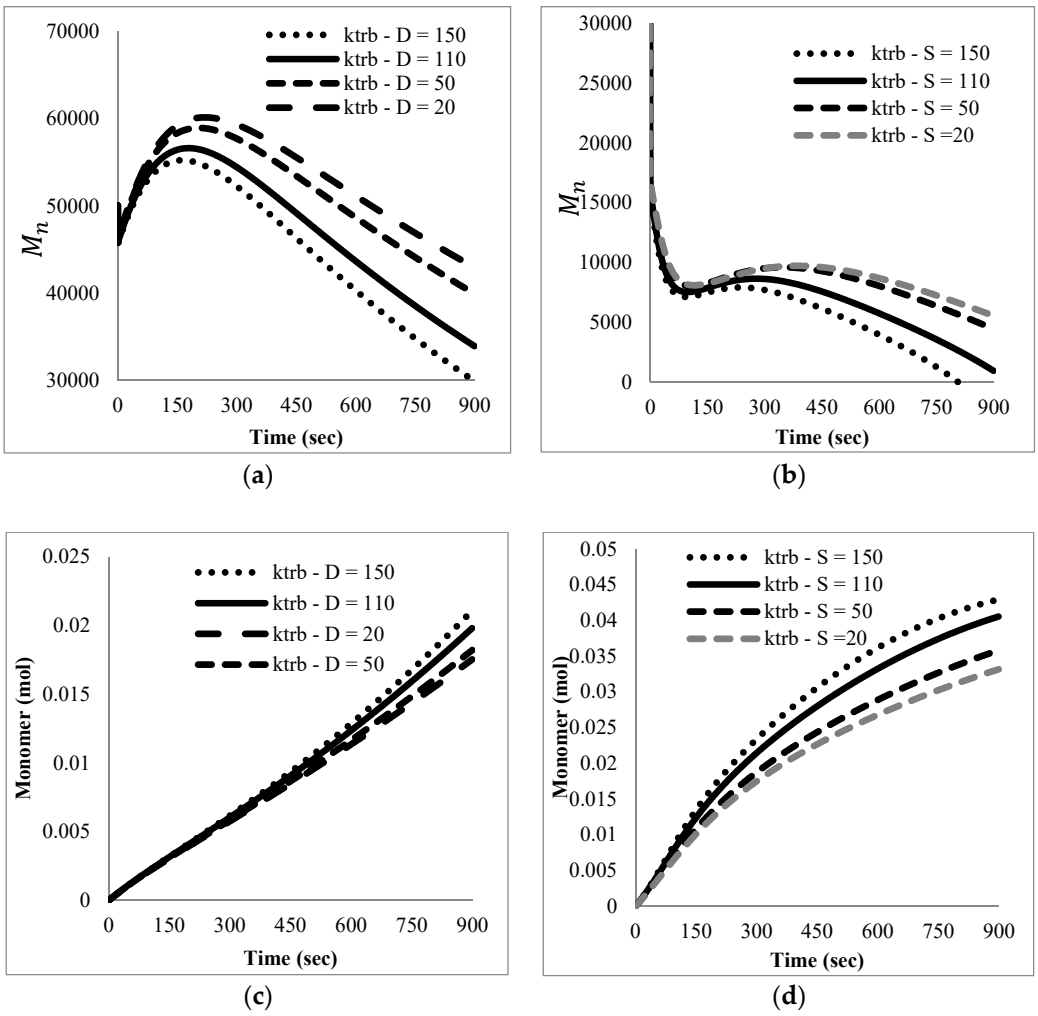

Figure 8. Effect of the variation of transfer to polymer + β-scission (k_{trb}) values on the pyrolysis M_n evolution of (**a**) dead polymer and (**b**) dormant polymer, and on the monomer generation of (**c**) dead polymer and (**d**) dormant polymer.

Remarkably, no reasonable results can be obtained by using typical values of this coefficient at temperatures in the range of 100–200 °C, which are in the order of 10^8 $Lmol^{-1}s^{-1}$ [40] and much lower values had to be used in the simulations; otherwise numerical convergence for the solution of the equations was not possible. Some researchers that have modeled the thermal pyrolysis of PS omit this reaction [41] at all; others, for example Kruse et al. [37,38], use a standard Arrhenius expression for this constant extrapolating its value at the high pyrolysis temperatures; however, they report to have used a gel effect expression modifying the Arrhenius expression which would lower the value of k_{tc} by several orders of magnitude. They do not report the resulting range of values for this constant,

but they may lie close to the values used in this work. Since it is not clear that diffusion limitations are present at these conditions, it was preferred here not to speculate and use instead a constant value that was adequate for the numerical solution of the model and resulted in reasonable outputs. In our next study this issue will be explored further.

In Figure 10 the effect of the reverse propagation value (k_{rev}) over the M_n evolution is shown. As for other parameters, for example those shown in Figures 7 and 8, the pyrolysis process for the dormant polymer is faster than for the dead polymer. The dormant polymer swiftly reaches a very low value of M_n, which is lower the higher the value of k_{rev}, while for dead polymer the value of M_n exhibits a gradually decreasing value even at the final time of the process. The generation of monomer in both cases is consistent with the decrease of the molecular weight.

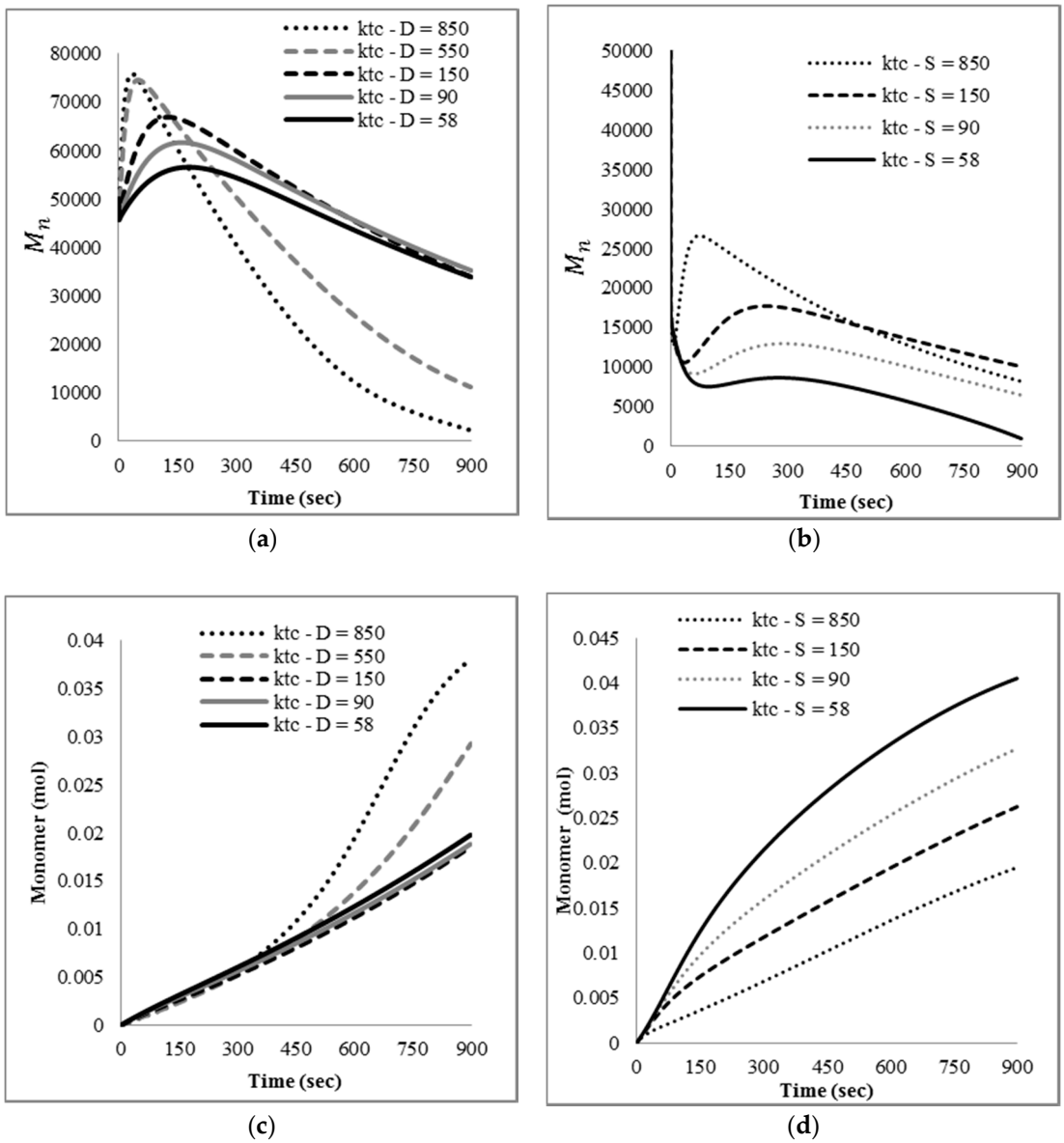

Figure 9. Effect of the variation of the termination by combination coefficient, k_{tc}, value on the pyrolysis M_n evolution of (**a**) dead polymer and (**b**) dormant polymer, and on the monomer generation of (**c**) dead polymer and (**d**) dormant polymer.

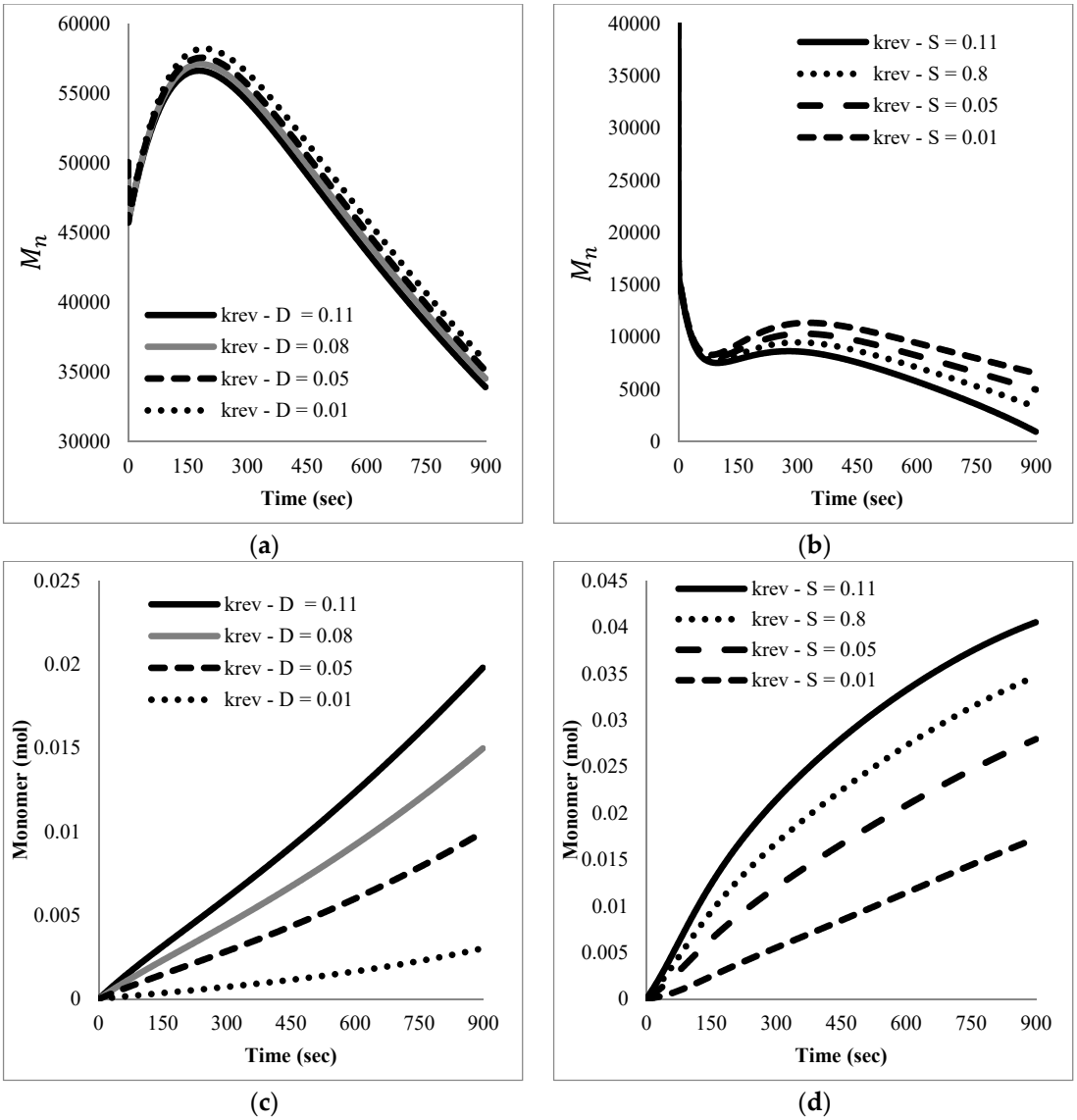

Figure 10. Effect of the variation of the reverse propagation coefficient value, k_{rev}, on the pyrolysis M_n evolution of (**a**) dead polymer and (**b**) dormant polymer, and on the monomer generation of (**c**) dead polymer and (**d**) dormant polymer.

The sensitivity of the outputs to k_{td} is not included here since it results in effects closely related to those observed with k_{tc}.

Figure 11 shows the effect of the mid-chain random scission value (k_b) on the number average molecular weight and monomer generation evolution. Mid-chain β-scission has been identified as a key step in the reduction of molecular weight of polymers, resulting in the formation of an end-chain polymer radical and a stable polymer with a double bond at the chain end and it is considered a major contribution to the formation of styrene monomer from PS. [42] In the sensitivity calculations for the dead polymer case the behavior is somewhat complex and non-linear, but the magnitude of the effects are relatively small. These small effects, combined with the fact that the M_n value combines the populations of live and dead polymer, partly explains the complexity observed. Notice that the use of k_b values, far from those shown in Figure 11, resulted in no convergence of the integration algorithm; therefore, the values studied were restricted to a small range. On the other hand, for the dead polymer case, the monomer generation grows with an increase in the values of k_b, as expected. With respect to the dormant polymer case, the behavior of M_n is simpler, as this output decreases faster the larger

the value of k_b, as it could be expected; it seems that the presence of the activation reaction at the nitroxide end helps in removing small non-linear effects. Consistent with this behavior, the generation of monomer increases with larger values of k_b.

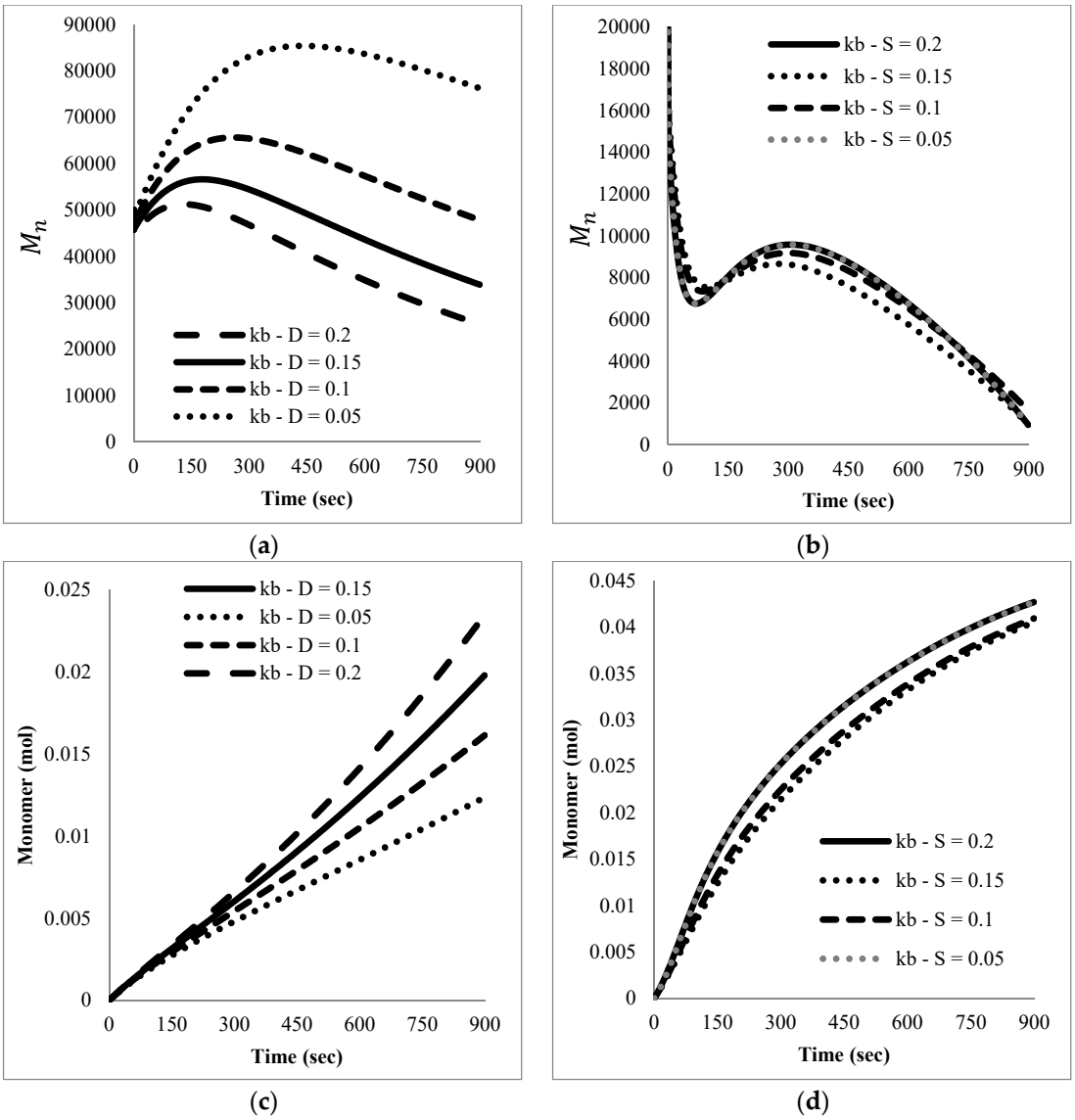

Figure 11. Effect of the variation of the mid-chain random scission coefficient, k_b, value on the pyrolysis M_n evolution of (**a**) dead polymer and (**b**) dormant polymer, and on the monomer generation of (**c**) dead polymer and (**d**) dormant polymer.

Notice that in all of the previous analyzed figures, the values of the constants tested can vary by several orders of magnitude, with no clear indication as to why the curves for the shown values were selected. The general criterion used to show curves for specific ranges of values of the kinetic constants was to maximize the sensitivity of the model to the parameters analyzed; that is, the curves were more sensitive for the ranges of values shown, and for others not shown the sensitivity was very small or almost null.

4.2. Base Case Simulation

As discussed before, given the difficulties to fit kinetic parameters for this system and the lack of detailed quantitative information from experiments, no attempt was made to compare in detail the

simulations with the experimental data. The goal at this stage was just to obtain agreement of the simulations with gross measurements of reaction progress, specifically the monomer generation and the time of reaction. In this section simulation results for the base case are presented and discussed. In a more detailed study, it would be convenient to gather data of M_n evolution with time, but this is experimentally difficult as it implies sampling in rather short reaction times and separate the polymeric species from the reaction mixture. This will be attempted in a future study. Figures 12 and 13 show the outputs of the simulations with the base case. The base case was assumed to have a M_n of 50,000 with dispersity of 1.9 (same as the FRP case in Table 1). For the dormant polymer a livingness of 100% was assumed. As commented above, the goal was to find a set of kinetic parameters that at least semi-quantitatively could reproduce the observed experimental trends; in particular, the decrease of M_n and the generation of around 30–40 wt.% of monomer. Figure 12 shows the decrease of M_n (a) for both the dead and the dormant polymer cases, as well as the generation of monomer (b). The M_n produced from the degradation of dormant polymer goes down to very low values, while that produced from dead polymer remains relatively high (around 35,000), although, as discussed below, this is mainly live polymer in relatively low concentration. More monomer is generated in the case of dormant polymer, as experimentally observed; out of the initial polymer present, the model predicts the conversion to monomer of about 43% (vs. 38.5% experimental) of the total polymer for the pyrolysis of dormant polymer (0.092 initial moles expressed as moles of monomer in the polymeric chain), and of 23% for the pyrolysis of dead polymer (vs. 33% experimental). The difference only qualitatively agrees with the experimental observation; the quantitative deviation can be explained by the oversimplification of the model with respect to the final small molecules formed, such as styrene dimers and trimers, which are not explicitly taken into account in the model, in particular when they are formed by recombination of monomer molecules.

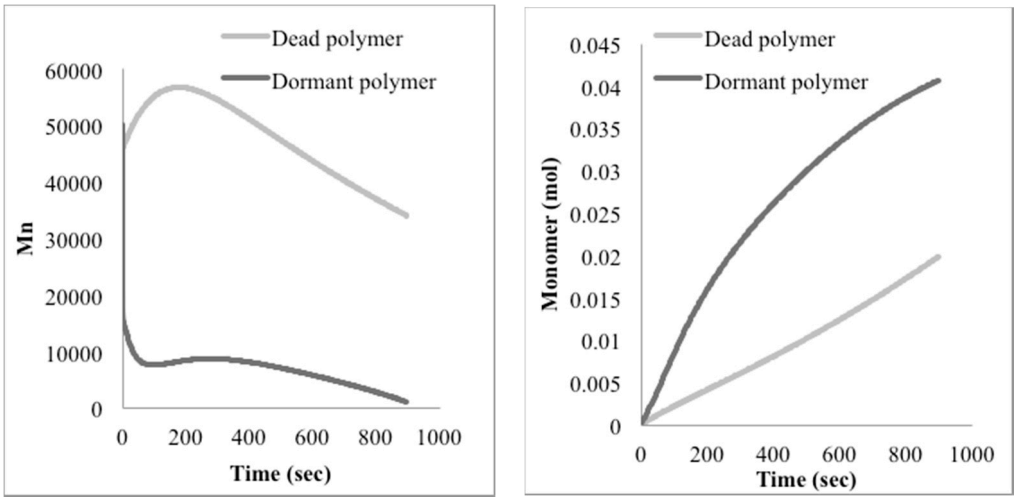

Figure 12. (**a**) M_n evolution, and (**b**) monomer generation for the pyrolysis of dead and dormant polymer predicted by the model with the base set of kinetic constants of Table 5.

Figure 13a,b show the predicted evolution of live and dead polymer concentration (zero-th moment) and of the first moments for both populations during the pyrolysis of dead polymer, indicating that the model predicts a very rapid activation of the dead polymer in the first instants of the reaction followed by reverse propagation and mid-chain breaking reactions. Initially, the first moment of dead polymer is around 0.092 mol, but this is not visible in plot (b) because in less than 1 s this polymer is activated and converted into live (activated) polymer which is gradually degraded. Similarly, plots (c) and (d) show the predicted evolution of the zero-th and first moments, respectively, of the four polymer populations existing during the pyrolysis of dormant polymer. Although more

complex than in the former case, the overall dynamics of the process are equivalent. Looking at plot (d) all the dormant polymer is rapidly converted into live polymer or live polymer with a nitroxide-end, and these two populations undergo reverse propagation decaying gradually, but faster than in the case of dead polymer pyrolysis. In the process some dead polymer is formed, but in concentrations several orders of magnitude lower than the live polymer.

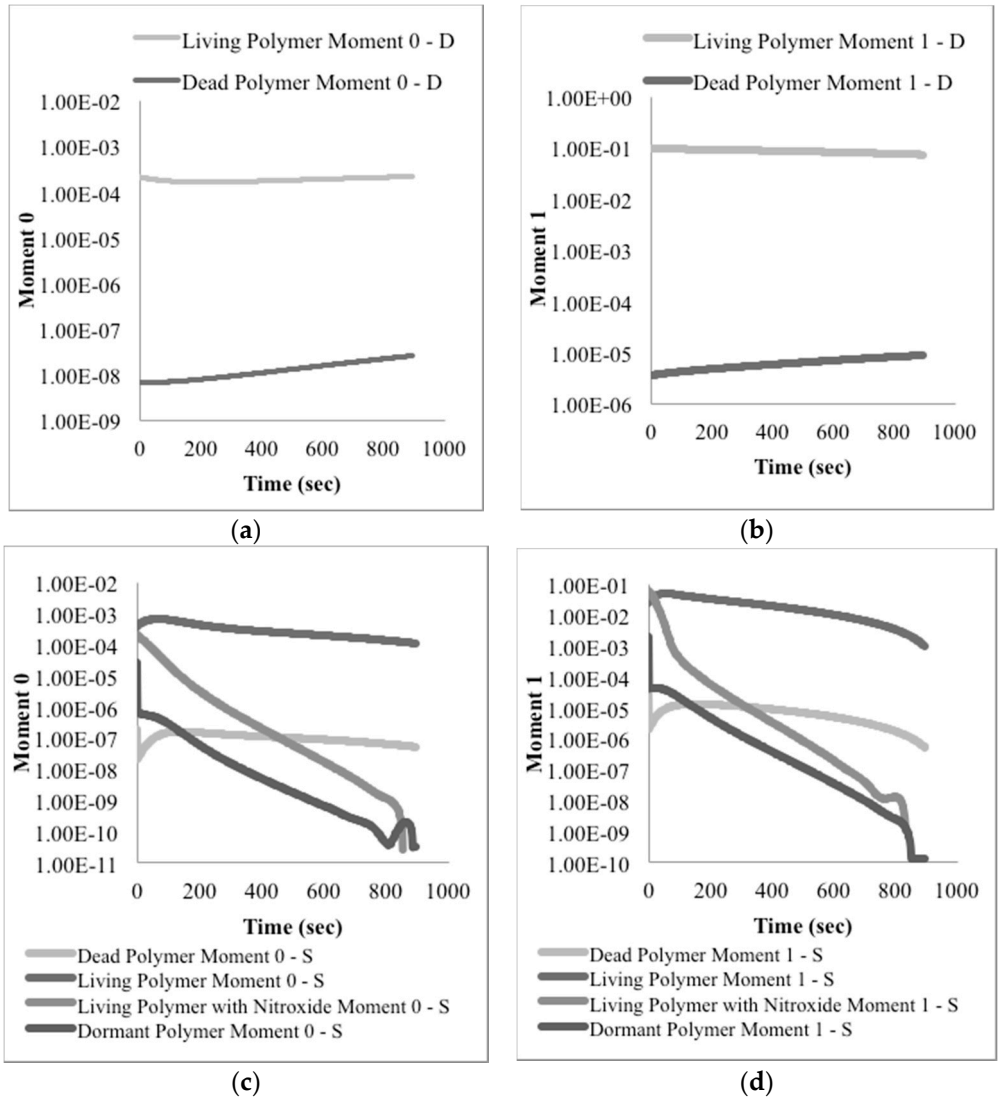

Figure 13. Model predictions for (**a**) zero-th moment evolution and (**b**) first moment evolution of live and dead polymer for the pyrolysis of dead PS. Also, model predictions for (**c**) zero-th moment evolution and (**d**) first moment evolution of live, dead, dormant, and live with a nitroxide-end polymer starting from dormant PS.

5. Conclusions

A simple process for the thermal pyrolysis of PS has been presented. PS-T (dormant PS) undergoes thermal pyrolysis and monomer formation more effectively than conventional (dead) PS, presumably due to the additional activation produced at the nitroxide end at temperatures above the T_c of PS, supporting the hypothesis of this work. With the nitroxide-functionalized PS the monomer production increases from ~33 to ~38.5 wt.% with respect to the initial polymer, an efficiency enhancement of roughly 15–16%. A kinetic and mathematical model was developed to explain the observed differences, and, after some parameter fitting, the model is capable of produce semi-quantitative agreement with

the experimental observations regarding time of reaction and monomer production, starting either from dead or dormant polymer. It is a difficult task to develop a predictive model for polymer pyrolysis due the complex polymer structure, the multiple reactions that take place and the large amount of intermediate compounds with different size and compositions that are formed in this intricate process, but with the help of population balance equations and the method of moments it is in principle possible to track the formation of the pyrolysis products and, in particular, the evolution of monomer.

Author Contributions: Conceptualization and methodology, E.S.-G., A.O.-Q. and A.M.-A.; software, E.S.-G. and A.O.-Q.; validation, A.M.-A. and A.O.-Q.; formal analysis, E.S.-G.; resources, E.S.-G.; writing—original draft preparation, A.O.-Q. and E.S.-G.; writing—review and editing, E.S.-G. All authors have read and agreed to the published version of the manuscript.

Funding: This research was partially funded by Consejo Nacional de Ciencia y Tecnología México (CONACYT), grant numbers 256358 and 278829.

Conflicts of Interest: The authors declare no conflict of interest.

References

1. Saldívar-Guerra, E.; Vivaldo-Lima, E. Polymers and polymer types. In *Handbook of Polymer Synthesis, Characterization and Processing*; Chapter 1; Saldívar-Guerra, E., Vivaldo-Lima, E., Eds.; John Wiley and Sons: Hoboken, NJ, USA, 2013.
2. McCrum, N.G.; Buckley, C.P.; Bucknall, C.B. *Principles of Polymer Engineering*, 2nd ed.; Chapter 1; Oxford Science Publications: Oxford, UK, 1997.
3. Villalobos, M.A.; Debling, J. Bulk and solution processes. In *Handbook of Polymer Synthesis, Characterization and Processing*; Chapter 13; Saldívar-Guerra, E., Vivaldo-Lima, E., Eds.; John Wiley and Sons: Hoboken, NJ, USA, 2013.
4. Tullo, A.H. Fighting ocean plastics at the source. *Chem. Eng. News* **2018**, *96*, 28–34.
5. Scott, A. Not-so-fantastic plastic. *Chem. Eng. News* **2018**, *96*, 16–18.
6. Achilias, D.S.; Andriotis, L.; Koutsidis, I.A.; Louka, D.A.; Nianias, N.P.; Siafaka, P.; Tsagkalias, I.; Tsintzou, G. Recent advances in the chemical recycling of polymers (PP, PS, LDPE, HDPE, PVC, PC, Nylon, PMMA). In *Material Recycling Trends and Perspectives*; Achilias, D., Ed.; InTechOpen: London, UK, 2012.
7. Al-Salem, S.M.; Antelava, A.; Constantinou, A.; Manos, G.; Dutta, A. A review on thermal and catalytic pyrolysis of Plastic Solid Waste (PSW). *J. Environ. Manag.* **2017**, *197*, 177–198. [CrossRef] [PubMed]
8. David, C. Thermal degradation of polymers. In *Comprehensive Chemical Kinetics*; Bamford, C.H., Tipper, C.F.H., Eds.; Elsevier Scientific Publishing Company: New York, NY, USA, 1957; Volume 14, pp. 1–173.
9. Guyot, A. Recent developments in the thermal degradation of polystyrene—A review. *Polym. Degrad. Stab.* **1986**, *15*, 219–235. [CrossRef]
10. Grassie, N.; Kerr, W.W. The thermal depolymerization of polystyrene. Part 1—The reaction mechanism. *Trans. Faraday Soc.* **1957**, *53*, 234–239. [CrossRef]
11. Faravelli, T.; Bozzano, G.; Colombo, M.; Ranzi, E.; Dente, M. Kinetic modeling of the thermal degradation of polyethylene and polystyrene mixtures. *J. Anal. Appl. Pyrolysis* **2003**, *70*, 761–777. [CrossRef]
12. Malhotra, S.L.; Hesse, J.; Blanchard, L.P. Thermal decomposition of polystyrene. *Polymer* **1975**, *16*, 81–93. [CrossRef]
13. Lehrle, R.S.; Peakman, R.E.; Robb, J.C. Pyrolysis-gas-liquid-chromatography utilised for a kinetic study of the mechanisms of initiation and termination in the thermal degradation of polystyrene. *Eur. Polym. J.* **1982**, *18*, 517–529. [CrossRef]
14. Madorsky, S.L. Rates of thermal degradation of polystyrene and polyethylene in a vacuum. *J. Polym. Sci.* **1952**, *9*, 133–156. [CrossRef]
15. Guaita, M. Thermal degradation of polystyrene. *Br. Polym. J.* **1986**, *18*, 226–230. [CrossRef]
16. Odian, G. *Principles of Polymerization*; John Wiley & Sons, Inc.: Hoboken, NJ, USA, 2004.
17. Stevens, M.P. *Polymer Chemistry: An Introduction*, 3rd ed.; Oxford University Press: New York, NY, USA, 1999.
18. Audisio, G.; Bertini, F. Molecular weight and pyrolysis products distribution of polymers. I. Polystyrene. *J. Anal. Appl. Pyrolysis* **1992**, *24*, 61–74. [CrossRef]

19. Beyler, C.L.; Hirschler, M.M. Beyler_Hirschler_SFPE_Handbook_3. In *SFPE Handbook of Fire Protection Engineering*; National Fire Protection Association: Quincy, MA, USA, 2002; pp. 111–131.
20. Liu, Y.; Qian, J.; Wang, J. Pyrolysis of polystyrene waste in a fluidized-bed reactor to obtain styrene monomer and gasoline fraction. *Fuel Process. Technol.* **2000**, *63*, 45–55. [CrossRef]
21. Simard, Y.D.M.; Kamal, M.R.; Cooper, D.G. Thermolysis of Polystyrene. *J. Appl. Polym. Sci.* **1995**, *58*, 843–851. [CrossRef]
22. Jellinek, H.H.G. Thermal degradation of polystyrene and polyethylene. Part III. *J. Polym. Sci.* **2003**, *4*, 13–36. [CrossRef]
23. Ebert, K.H.; Ederer, H.J.; Schroder, U.K.O.; Hamielec, A.W. On the kinetics and mechanism of thermal degradation of polystyrene. *Makromol. Chem.* **1982**, *183*, 1207–1218. [CrossRef]
24. Richards, D.H.; Salter, D.A. Thermal degradation of vinyl polymers II—The synthesis and degradation of polystyrene containing thermally weak bonds. *Polymer* **1967**, *8*, 139–152. [CrossRef]
25. Anderson, D.A.; Freeman, E.S. The kinetics of the thermal degradation of polystyrene and polyethylene. *J. Polym. Sci.* **1961**, *54*, 253–260. [CrossRef]
26. Wegner, J.; Patat, F. Thermal degradation of polystyrene. *J. Polym. Sci. Part C* **1970**, *31*, 121–135. [CrossRef]
27. Paisley, M.A.; Litt, R.D. Monomer Recovery from Polymeric Materials. U.S. Patent 5,326,919, 5 July 1994.
28. Luo, X.; Yie, F.; Tan, W. Method for Retrieving Styrene Monomer from Discarded Polystyrene Scrap through Pyrolytic Reduction. U.S. Patent 5,072,068, 10 December 1991.
29. Lee, S.; Gencer, M.A.; Fullerton, K.L.; Azzam, F.O. Depolymerization Process. U.S. Patent 5,386,055, 31 January 1995.
30. Tippet, J.; Butler, J.; Assef, J.; Ashbaugh, J.; Clark, J.; Duc, M.; Cary, J.-B. Depolymerization of Plastic Materials. U.S. Patent 9,650,313, 15 May 2017.
31. Northemann, A. Recovery of Styrene from Waste Polystyrene. U.S. Patent 5,672,794, 30 September 1997.
32. Yoon, B.T.; Choi, M.J.; Kim, S.B.; Lee, S.B. Method for Preparing Fermentable Sugar from Wood-Based Biomass. U.S. Patent 8,449,725, 24 March 2013.
33. Nicolas, J.; Guillaneuf, Y.; Lefay, C.; Bertin, D.; Gigmes, D.; Charleux, B. Nitroxide-mediated polymerization. *Prog. Polym. Sci.* **2013**, *38*, 63–235. [CrossRef]
34. Roland, A.I.; Schmidt-Naake, G. Thermal degradation of polystyrene produced by nitroxide-controlled radical polymerization. *J. Anal. Appl. Pyrolysis* **2001**, *58–59*, 143–154. [CrossRef]
35. Saidel, G.M.; Katz, S. Dynamic analysis of branching in radical polymerization. *J. Polym. Sci. Part A-2* **1968**, *6*, 1149–1160. [CrossRef]
36. Marongiu, A.; Faravelli, T.; Ranzi, E. Detailed kinetic modeling of the thermal degradation of vinyl polymers. *J. Anal. Appl. Pyrolysis* **2007**, *78*, 343–362. [CrossRef]
37. Kruse, T.M.; Woo, O.S.; Broadbelt, L.J. Detailed mechanistic modeling of polymer degradation: Application to polystyrene. *Chem. Eng. Sci.* **2001**, *56*, 971–979. [CrossRef]
38. Kruse, T.M.; Woo, O.S.; Wong, H.W.; Khan, S.S.; Broadbelt, L.J. Mechanistic modeling of polymer degradation: A comprehensive study of polystyrene. *Macromolecules* **2002**, *35*, 7830–7844. [CrossRef]
39. Lemoine-Nava, R.; Flores-Tlacuahuac, A.; Saldívar-Guerra, E. Optimal operating policies for the nitroxide-mediated radical polymerization of styrene in a semibatch reactor. *Ind. Eng. Chem. Res.* **2006**, *45*, 4637–4652. [CrossRef]
40. Beuermann, S.; Buback, M. Rate coefficients of free-radical polymerization deduced from pulsed laser experiments. *Prog. Polym. Sci.* **2002**, *27*, 191–254. [CrossRef]
41. Sterling, W.J.; Walline, K.S.; McCoy, B.J. Experimental study of polystyrene thermolysis to moderate conversión. *Polym. Degrad. Stabil.* **2001**, *73*, 75–82. [CrossRef]
42. Simha, R.; Wall, L.A.; Blatz, P.J. Depolymerization as a chain reaction. *J. Polym. Sci.* **2003**, *5*, 615–632. [CrossRef]

© 2020 by the authors. Licensee MDPI, Basel, Switzerland. This article is an open access article distributed under the terms and conditions of the Creative Commons Attribution (CC BY) license (http://creativecommons.org/licenses/by/4.0/).